# NITROGEN INJECTION INTO THE BASE REGION OF A HYPERSONIC WAKE

Thesis by
Robert T. Herzog

In Partial Fulfillment of the Requirements

For the Degree of

Aeronautical Engineer

California Institute of Technology
Pasadena, California
1964

## ACKNOWLEDGEMENTS

The author wishes to express his appreciation to Professor Lester Lees, Dr. Toshi Kubota and Dr. Eward Zukoski for their guidance and assistance through the course of this investigation; to Dr. Forbes Dewey, Jr. for suggesting the study; to Mr. Paul Baloga and the staff of the hypersonic laboratory for their expert assistance in conducting the experiment; and to the Aeronautics machine shop for constructing models and probes. He wishes to thank Miss Kikuko Matsumoto for writing the computer programs, Mr. Gerrit van Halewijn for preparing the figures, Mrs. Truus van Harreveld for preparing the graphs and Mrs. Katherine Cassady for typing the manuscript.

# ABSTRACT

An experimental investigation was made of the changes occurring in the near wake of a cylinder at M = 6.0 when nitrogen was injected into the base region. The free stream Reynolds number based on cylinder diameter was 30,000 and the rate of injection was varied from zero to 3 percent of the frontal area free stream mass flow. Pitot pressure profiles across the wake, Schlieren photographs and measurement of the boundary layer separation point on the cylinder were used to define the changes in wake geometry. Static pressure and temperature surveys were made along the wake centerline starting at the base of the cylinder and continuing downstream to X/D = 6.0. The injection reduced the recompression in the neck region and left only a slight isentropic compression in place of the strong wake shock. The recirculation of mass in the base region was eliminated with approximately 1.5 percent injection.

An automated hot wire recording system which produced data suitable for computer reduction was developed and used to measure temperature. In order to reduce the measured wire temperature to total temperature an attempt was made to use a previously developed computer program. Deficiencies in this program are discussed with suggestions for improvements.

# TABLE OF CONTENTS

# LIST OF FIGURES

# LIST OF SYMBOLS

| | |
|---|---|
| $d$ | hot wire diameter |
| $D$ | diameter of cylinderical model |
| $I$ | wire current |
| $k_o$ | thermal conductivity of air at temperature $T_o$ |
| $k_w$ | thermal conductivity of wire at temperature $T_w$ |
| $\ell$ | length of hot wire |
| $M$ | Mach number |
| $Nu_m$ | Nusselt number measured with finite length wire |
| $Nu_o$ | Nusselt number for infinite length wire |
| $p_o$ | reservoir pressure |
| $p_s$ | local static pressure |
| $p_{t_2}$ | pitot pressure |
| $q$ | heat transfer rate per unit area |
| $R$ | gas constant |
| $R_{awm}$ | resistance of hot wire at zero current |
| $R_m$ | resistance of hot wire with current flow |
| $R_r$ | resistance of hot wire at $0^oC$ zero current |
| $Re_D$ | Reynolds number of model $\rho_\infty U_\infty D/\mu_\infty$ |
| $Re_o$ | Reynolds number of hot wire $\rho Ud/\mu_o$ |
| $s$ | resistance parameter $\alpha_r T_o/\left[1 + \alpha_r(T_{awm} - T_r)\right]$ |
| $t_s$ | non-dimensional support temperature $\left[T_s - T_{awm}\right]/T_o$ |
| $T_{awm}$ | measured hot wire temperature extrapolated to zero current |
| $T_r$ | reference temperature $= 0^oC$ |

| | |
|---|---|
| $T_{RES}$ | reservoir temperature |
| $T_s$ | temperature of hot wire supports |
| $T_{wm}$ | measured wire temperature |
| $T_o$ | local total temperature |
| $T_*$ | recovery temperature for infinite length wire |
| $U_\infty$ | free stream velocity |
| X | distance from cylinder axis in streamwise direction |
| Y | distance from cylinder axis in transverse direction |
| $\alpha_r$ | temperature resistance coefficient (Eq. 3.1) |
| $\gamma$ | ratio of specific heats |
| $\eta_c$ | recovery ratio for continuum flow |
| $\eta_f$ | recovery ratio for free molecular flow |
| $\eta_*$ | recovery ratio for wire of infinite length |
| $\bar{\eta}_*$ | normalized recovery ratio $(\eta - \eta_c)/(\eta_f - \eta_c)$ |
| $\rho_\infty$ | free stream density |
| $\psi_R$ | end loss correction factor for recovery ratio |
| $\psi_N$ | end loss correction factor for Nusselt number |
| $\mu_\infty$ | viscosity of air at free stream temperature |
| $\mu_o$ | viscosity of air at $T_o$ |

# I. INTRODUCTION

The development of inter-continental ballistic missiles and hypersonic re-entry vehicles has created considerable interest in the study of hypersonic wakes. Previous theoretical and experimental investigations have shown the existence of a recirculation region in the near wake which influences the wake characteristics. The recirculation is the result of the free shear layer entraining mass from the base region which then must be returned for mass conservation. A pressure rise in the neck region is associated with the momentum balance which causes the reverse flow of mass along the wake centerline. If sufficient mass were injected into the base region there would be no recirculation region and consequently no recompression. Present theoretical knowledge does not allow determination of the precise amount of injection required to eliminate recirculation, because of uncertainties in the initial free shear layer and the exact mixing process. Therefore, an experimental program was initiated: its primary objective was to investigate the effects of nitrogen injection at the base of a cylinder spanning the GALCIT hypersonic tunnel (M = 6); a secondary objective became the automation and improvement of hot wire anemometer techniques for local subsonic and supersonic flow.

A systematic study of hypersonic wakes has been in progress at GALCIT for several years. Theoretical studies have been made by

Chapman (1, 2, 3, 4)*, Lees (5, 6), Hromas (6) and Kubota (7). Experimental investigations were conducted by Mohlenhoff (8), Kingsland (9), Demetriades (10), McCarthy (11) and Dewey (12, 13). The development of the hot wire anemometer as a flow measurement device was advanced by Dewey's (12) correlation of heat transfer data and development of a computer program for end loss corrections. It is this work that is the basis for the hot wire system used in this experiment.

---

* Numbers in parentheses denote references listed at end of text.

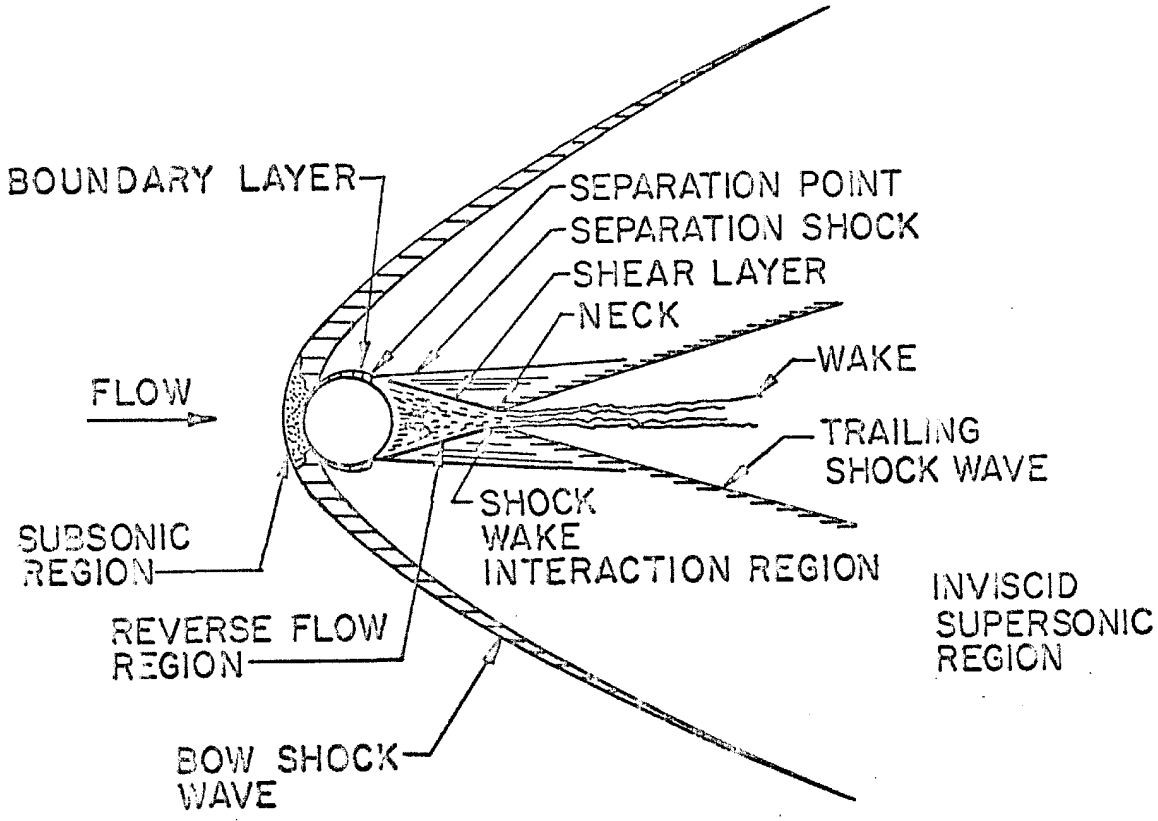


Fig. 1 Hypersonic Flow Field Around Cylinder

The model used was a 0.200 in. diameter cylinder with a porous ceramic port across the back for injection (Figure 2). The region investigated (Figure 1) extends across the wake and a distance of six diameters downstream from the center of the model.

Nitrogen was used for injection because it was a readily available source of high pressure dry gas with a thermal conductivity and molecular weight close to air. The injection rate is specified as:

$$\text{Injection Rate} = \frac{\dot{N}_{2\,\text{Mass Flow}}}{\rho_\infty U_\infty D\ (\text{Length}_{\text{Injection Port}})}$$

The injection rates used were 0, 1.0, 1.5, 2.0 and 3.0 percents. The flow field was first investigated with Schlieren photography to determine the major effects to be expected at different injection rates. This study was followed by a detailed investigation of the flow field using pitot pressure, static pressure, and hot wire measurements. In addition the movement of the boundary layer separation point on the cylinder was determined by visual measurement of the oil film on the model.

# II. EXPERIMENTAL APPARATUS AND PROCEDURES

## II. 1 Facilities

The experimental tests were conducted in Leg I of the GALCIT Hypersonic Wind Tunnel which is a closed return, continuous flow system. Leg I has fixed nozzle blocks which provide a 5" by 5.25" test section at a nominal Mach number of 6.0. The reservoir temperature and pressure are variable; however, all tests were conducted at 80 PSIA and 275°F (408°K) which produced a Reynolds number of 30,000 based on model diameter and free stream conditions. In selecting the operating conditions it was found to be desirable to use a high pressure to obtain sharp Schlieren photographs and more reliable pressure measurements. However, maximum reservoir pressures increased the incidence of hot wire breakage and increased the difficulty of obtaining high injection rates through the porous injection port.

A total pressure survey without the model installed was used to determine the uniformity of the flow field at the selected operating conditions. It was found that the Mach number varied smoothly from 6.08 at the normal model location to 6.15 at a point nine inches downstream (X/D = 45), at which point a noticeable pressure disturbance was observed. Reservoir pressure was controlled automatically to $\pm$ .02 PSIG and the gauge pressure was varied with barometric pressure to obtain 80.00 $\pm$ .02 PSIA. Reservoir temperature was regulated to $\pm$ 1°F with an automatic regulator which was calibrated

against an iron constantan thermocouple inserted into the reservoir one inch ahead of the throat.

II. 2 Model

Previous experiments in Leg I indicated that the largest cylinder that could be installed without encountering tunnel starting difficulties was 0. 2 inch. All models were made to this diameter because of the difficulty in machining smaller injection ports and to avoid reducing the dimensions of the flow field with respect to probe size. The models were made of stainless steel machined to the dimensions shown in Figure 2. The porous ceramic plug was cut from a section of alumina tubing similar to that used by Kingsland (9). It was cemented into the injection port with a minimum amount of Eccobond epoxy. After assembly the ceramic was ground to the radius of the model. One of the models was constructed with four base pressure taps located off centerline. This model gave only fair reliability due to the non-uniform injection around the cemented joints.

The glass ports on each side of the tunnel were used to support the model. A 0. 210 inch hole was bored into the center of each port and the joints between the model and the ports were sealed with a double sets of"0" rings. Rotational and longitudinal alignments were made by centering the injection port. The initial rotational alignment was accomplished using a traveling microscope and thereafter a

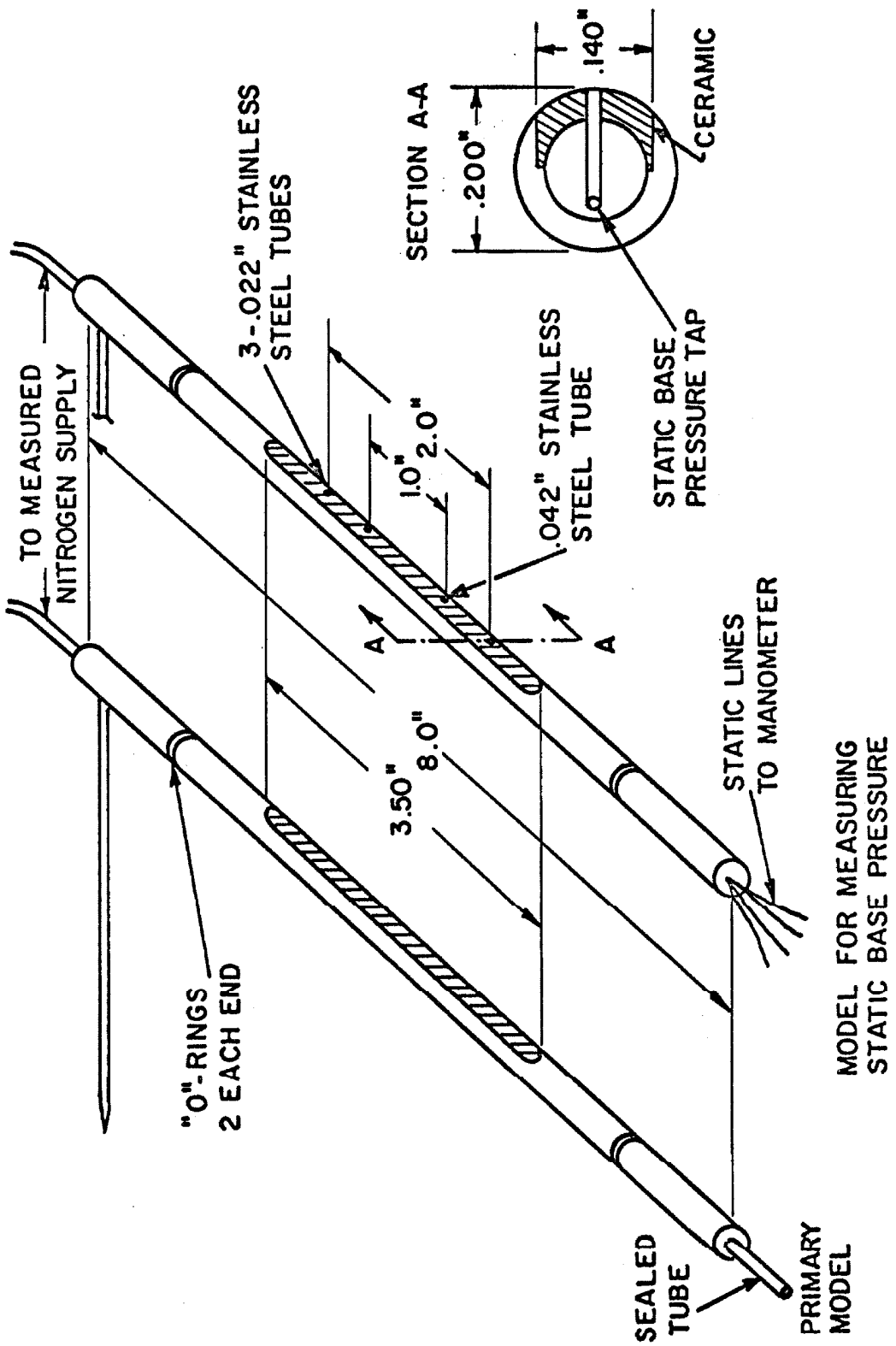


Fig. 2 Models Used for Base Flow Injection

pointer attached to the model was used. Preliminary checks of the flow field with Schlieren photography and a survey made with a total pressure probe showed that a $20^{o}$ rotation of the injection port varied the symmetry of the flow field only slightly.

## II. 3 Injection Control

The system used for regulating and measuring the flow of nitrogen is shown in Figure 3. The inlet pressure to the flow meter (Fischer-Porter Tri-flat FP 1/4-16-G-5) was maintained at 50 PSIG by the pressure regulator. Flow to the model was regulated by adjusting the needle valve on the exit side of the flow meter. The gas-temperature through the flow meter was measured with a standard mercury thermometer and found to remain within $25^{o}$ - $28^{o}$ C for all tests.

The entire system was calibrated by measuring the time it took to displace the water from an inverted 5 gallon water bottle. The neck of the bottle gave a very accurate measure of the exact volume. The density of the measured volume of gas was then calculated knowing the temperature, barometric pressure, and water vapor pressure. By calculating the complete system as a unit it was not necessary to calibrate each gauge in terms of absolute values provided the temperature of the gas remained relatively constant. A check on the repeatability of setting a given mass flow was made by conducting the calibration on two different days. It was found that the mass flow could be set to $\pm$ 0.5 percent of the full scale flow, (about 3% injection rate).

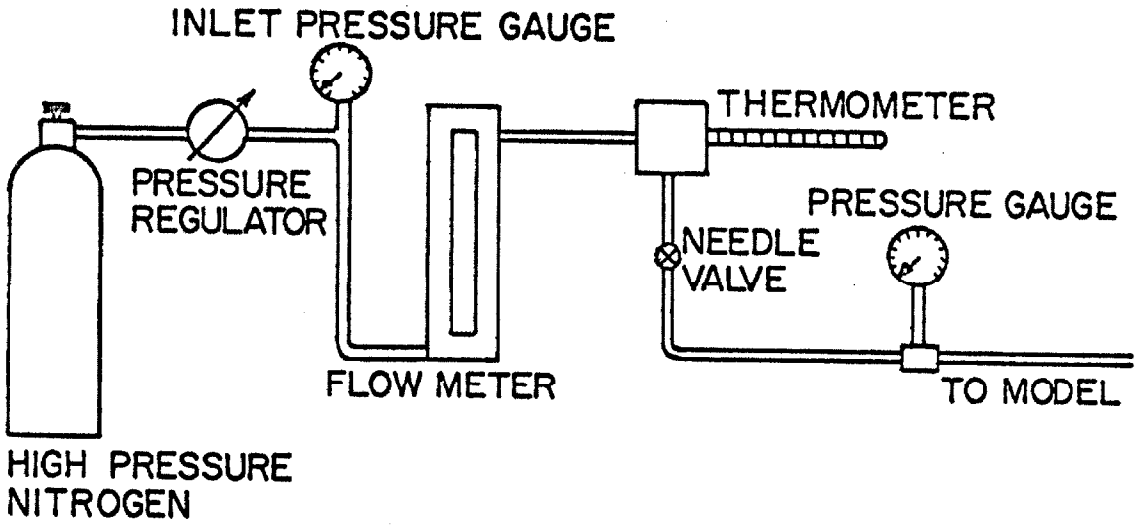


Fig. 3 Nitrogen Mass Injection Control and Measuring System

II. 4 Spanwise Uniformity

In his investigation using a porous cylinder for injection, Kingsland (9) found that he experienced non-uniform injection because of saturation from oil in the free stream. Therefore, the uniformity of nitrogen injection was checked before and after running the model by observing the formation of bubbles along the span of the model while it was submerged in water. The test showed good uniformity of injection, however, there was oil impregnation present as indicated by the gradual increase in pressure required to force the same flow of nitrogen through the ceramic port. To keep this impregnation to a minimum nitrogen was injected at all times the tunnel was operating, except when actually making a zero injection wake survey. The

primary reason for not experiencing the non-uniform oil impregnation can be attributed to the fact that the ceramic material covered only the region of separated flow and not the impact region on the front of the model.

An investigation of the spanwise flow was made by taking a pressure survey behind the model both with and without fences attached. The apparatus for making this survey is shown in Figure 4. Close to the model a rectangular (.008" x .050") pitot probe was used. It was oriented such that the flat of the probe was perpendicular to the direction of travel. Using this probe several profiles were taken at different injection rates and distances behind the model. At X/D = 2 the pitot probe began to pick up the flow in the shear layer and therefore a static probe was used further downstream. The pressure from the probes was measured by an electric transducer and used as the "Y" input signal to the X - Y recorder. The signal for the X axis was proportional to the probe spanwise position.

Fences were cut from .005" steel shim stock in the shape of an ellipse $1\frac{1}{2}$" long. A hole for the model was drilled at one end and the edges were ground sharp. The fences were then glued to the model at the edge of the injection port using radio cement on the side away from the port.

Some typical traces taken in this survey are shown in Figure 5. The non-uniformity immediately behind the model is due to the porous nature of the ceramic. However, this local non-uniformity died out rapidly and was not apparent at an X/D = 1 (0.1"behind model).

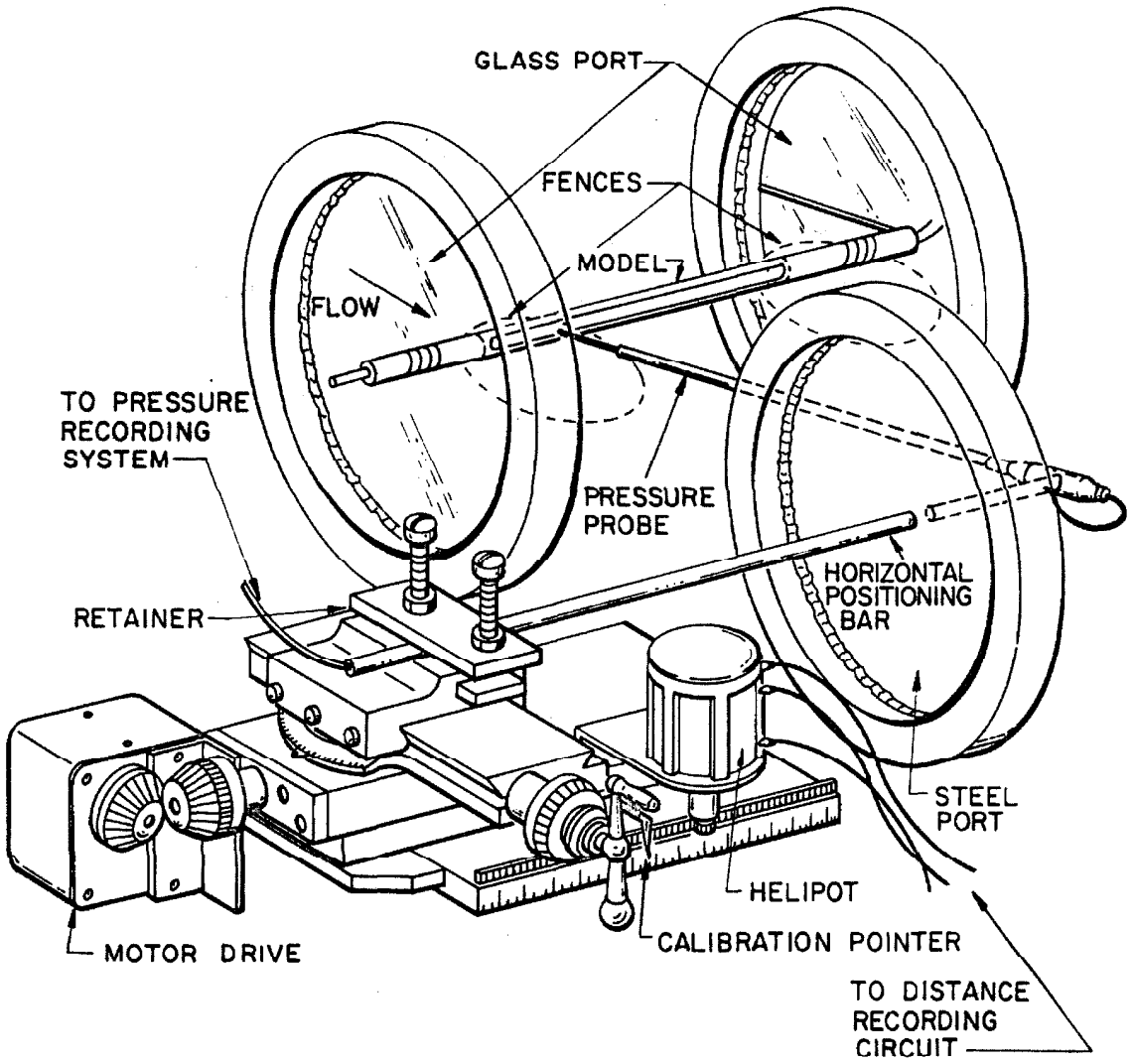


Fig. 4. Traversing Mechanism for Horizontal Pressure Survey

In comparing the pitot pressure traces with and without fences and at different injection rates it appears that there is no appreciable end loss into the tunnel boundary layer. The pitot pressure at the ends of the injection port is higher with the fences installed, but this can be attributed to an increase in static pressure similar to the change

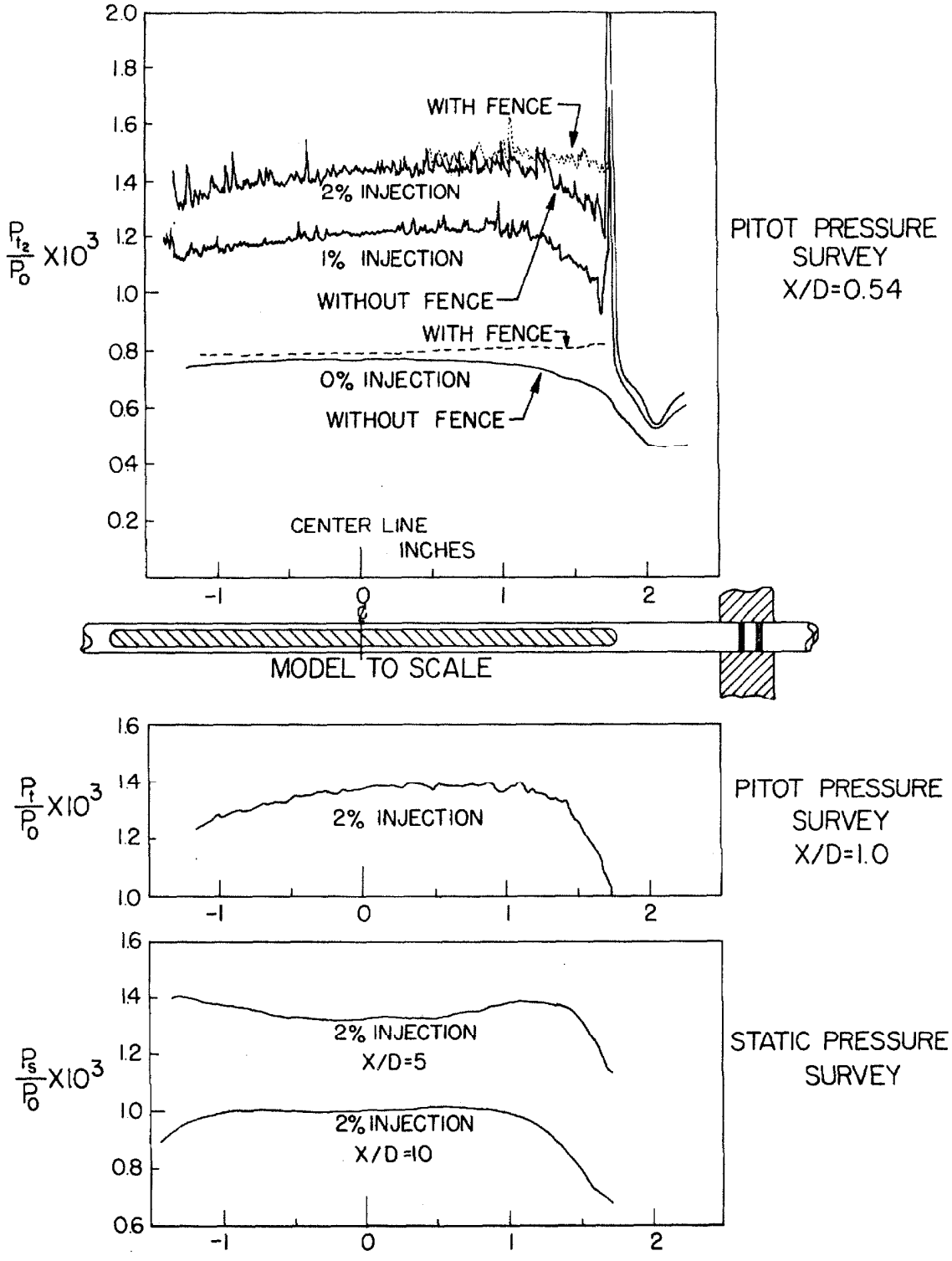


Fig. 5 Typical Results: Horizontal Pressure Survey

in static pressure distribution for the zero injection case. Another verification that large end losses do not exist is obtained by observing the geometry of the neck region beyond the end of the injection port. This region does not elongate with increased injection to the extent that the region behind the port does. This behavior indicates that a recirculation region still exists past the end of the injection port.

The uniformity of injection can be attributed to the high pressure drop across the ceramic material. This allows uniform distribution of nitrogen along the inside of the model and produces the same injection rate independent of base static pressure. This conclusion was made after observing that for a given flow meter setting the absolute mass flow of nitrogen remained constant while varying the tunnel operating pressure.

## II. 5 Pitot Pressure Measurements

A schematic diagram of the system used in measuring and recording the pitot pressure data is shown in Figure 6. The pitot pressure was measured with a pressure transducer. The output of the transducer was fed through a balance circuit to an amplifier and then to the "Y" axis of the X - Y plotter. The signal for the "X" axis was proportional to the position of the probe. This signal was obtained from a voltage divider network incorporating a potentiometer driven by the probe positioning mechanism. A rectangular pitot probe .008" thick and .052" wide was used to reduce the time constant while maintaining a reasonable degree of resolution within the shear layer.

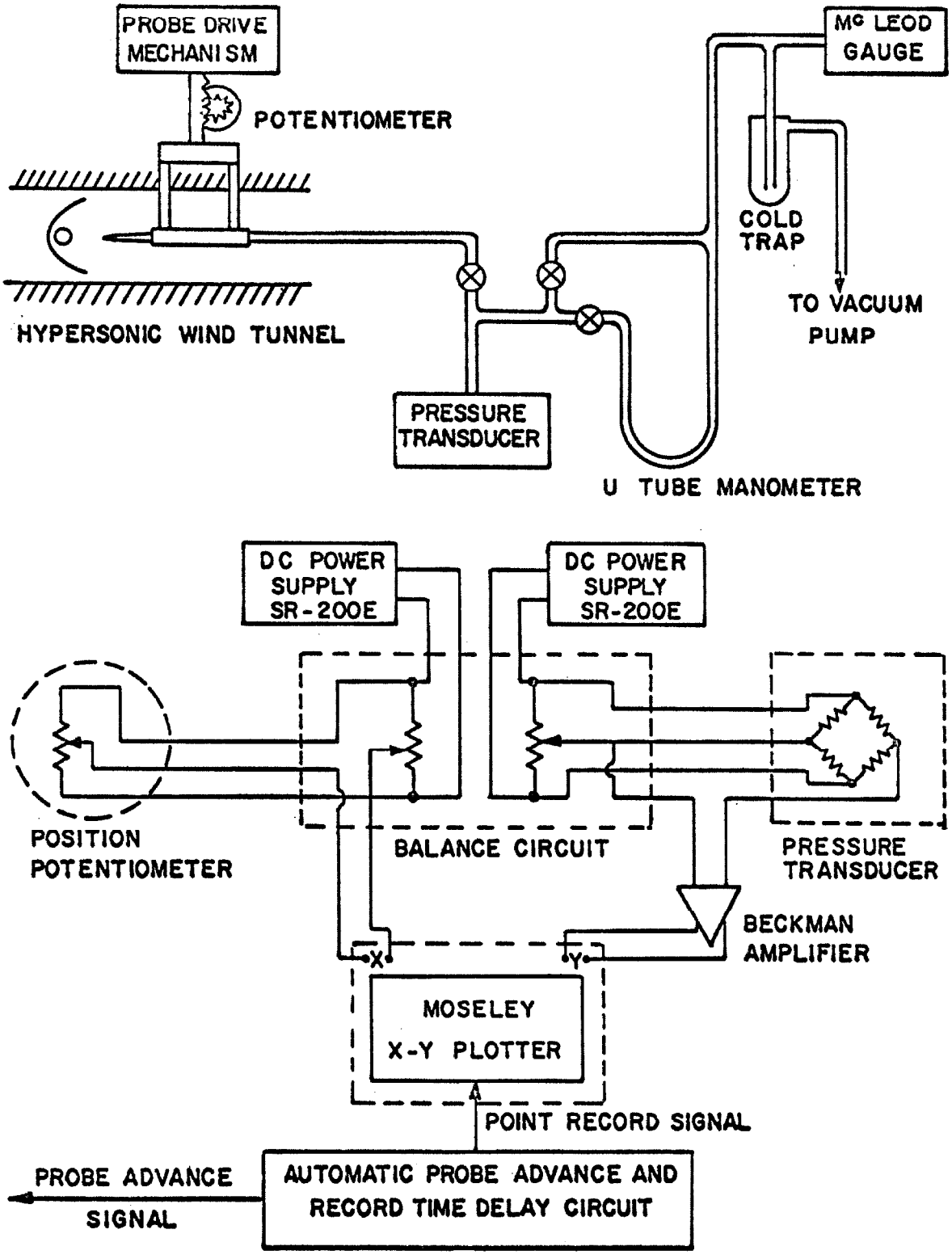


Fig. 6 Schematic of Pressure Measuring and Recording System

Since the inside dimension of the probe was only .004" the pneumatic response time of the probe, connecting line and transducer was on the order of 5 - 10 seconds. This lag necessitates a delay between positioning the probe and recording the data. The delay was obtained by constructing a unit which would automatically advance the probe, delay a set time, depress the recording pen, and then repeat the cycle. Both the probe advance distance and the delay time were variable and could be set by the operator.

The transducer used to measure the pressure was a Statham PA 208 TC-5-350 employing a compensated strain gauge bridge. This unit proved to be remarkably accurate. The unit was calibrated using a mercury manometer read with a traveling eye piece which made it possible to read differential pressures to $\pm$ .05 mm. The output of the transducer was measured using a Beckman amplifier and digital voltmeter. With this calibration system it was possible to read to an accuracy of .05 percent of full scale. A plot of results showed no deviation from a straight line. Numerical reduction of the calibration data showed a repeatability of better than $\pm$ 0.1 mm Hg.

The accuracy of the pressure recording system was not limited by the equipment but by the selection of a suitable scale which would allow measurement of the high pitot pressure outside the inner wake and yet give good resolution in the subsonic base region. To overcome this problem a survey of the entire wake was made using a suitable scale, and then centerline pressures were measured using a scale

amplification of ten times the original scale. In the latter case the pressures measured were on the order of 5.0 mm Hg, and considerable care had to be taken in balancing the transducer to the zero reference pressure. While the transducer was still linear and produced repeatable results, the zero balance varied because of changes in temperature of the transducer, and therefore it was balanced after every trace. The accuracy of the over-all flow field pressures was limited by ones ability to read the graph, which was about 0.3 percent of full scale deflection. The centerline pressure could be read to an accuracy of better than 1.0 percent of full scale deflection.

## II.6 Static Pressure Measurements

The static pressure was measured along the wake centerline and across the back of the model for each of seven different injection rates. The location of the static port on a conventional static probe limited its use to making measurements downstream of $X/D = 2$. The probe was .002" in diameter and had a $20^{o}$ nose cone. The static port was located 10 probe diameters from the cone. Static pressures ahead of $X/D = 2$ were measured by a similar probe which was inserted into the .042" base pressure tap on the model designed for base pressure measurements. The probe was sealed into the .042" tubing with Glyptal, allowed to dry under a heat lamp, and checked for leaks prior to testing. Tests were conducted at different injection rates, the probe was removed, shortened, and the procedure was

repeated. The static base pressure was measured across the span of the model using four base pressure taps as shown in Figure 2.

All static pressures were measured using a "U" tube manometer filled with silicon oil. The level of the fluid was measured with a traveling eye piece which permitted reading the pressure differential to $\pm$ .05 mm. The reference side of the manometer was maintained at 0.5 microns Hg. by use of a vacuum system incorporating both a diffusion pump and a mechanical vacuum pump.

Some difficulty was experienced with outgassing at first, but this was eliminated by switching to Saran tubing and keeping the system under vacuum prior to testing. Uncertainties in the exact probe location ($\pm$ .01") accounted for some of scatter in data when investigating regions of large pressure gradient in the downstream direction.

## II. 7 Separation Point Movement

The movement of the boundary layer separation point on the cylinder with changes in injection rate could be determined by visual observation of the oil film attached to the model. The oil film was not intentional but rather the result of oil deposited in the air supply by the compressors. While the oil was detrimental to the porous injection port and the quality of the Schlieren photographs it did prove a benefit in making visual observation of the separation point. A traveling microscope located outside the tunnel was used to measure the movement. The optical path of the microscope was at an angle

to the model axis and the plane of movement was tangent to the average separation point. Since the movement of the separation point around the cylinder was only $12^{o}$, the cosine error induced by measuring in a straight line was smaller than the accuracy with which the microscope travel could be read.

## II. 8 Hot Wire Measurements

Hot wire measurements were made with the intent of using them in conjunction with pitot pressure to define the flow in a manner suggested by Dewey (12). This approach was not satisfactory due to deficiencies in the computer reduction program which are discussed in Appendix B. To use the hot wire in measuring the local total temperature, $T_o$, the following information is required.

1. Resistance of the hot wire for different heating currents.
2. Temperature of the end supports.
3. A relationship between the above quantities to determine the adabatic recovery temperature a wire of "infinite" length in the same flow ($T_*$) .
4. A relation between the recovery temperature $T_*$ and total temperature $T_o$ .

In the present investigation the first two quantities were measured. The latter two were calculated using the relations determined by Dewey.

In his original work Dewey calculated the needle support temperature $T_s$ by assuming that it was .9030 ($T_o$). Although this approach proved applicable to free stream measurements it is not satisfactory when the supports move through a field in which a large gradient in $T_o$ exists. This conclusion was suggested by asymmetric variations in the hot wire data which changed when the rate of injection or speed of probe traverse was changed. A thermocouple was welded to the tip of one of the support needles and the support temperature was measured. The results of these measurements presented in Figure 7 show that the support temperature is not a constant times the measured local $T_o$. The asymmetry shown in this figure occurs because of the relatively high thermal conductivity of the needles which are located in a strong temperature gradient. The needles are attached to the probe at approximately a $20^o$ downward angle to the horizontal. In measuring the bottom part of the wake profile they extend through the wake centerline where a portion of the needle is cooled. Above the wake centerline none of the needle is cooled; therefore, an asymmetry occurs. It was found that there was also a time dependence based on the time it took the supports to reach thermal equilibrium.

Thermocouples were added to two of the hot wire probes developed by Dewey and these probes were used for all the final hot wire measurements. The thermocouples were made from .001" chromel and alumel wire welded to within .003" of the tip of one of

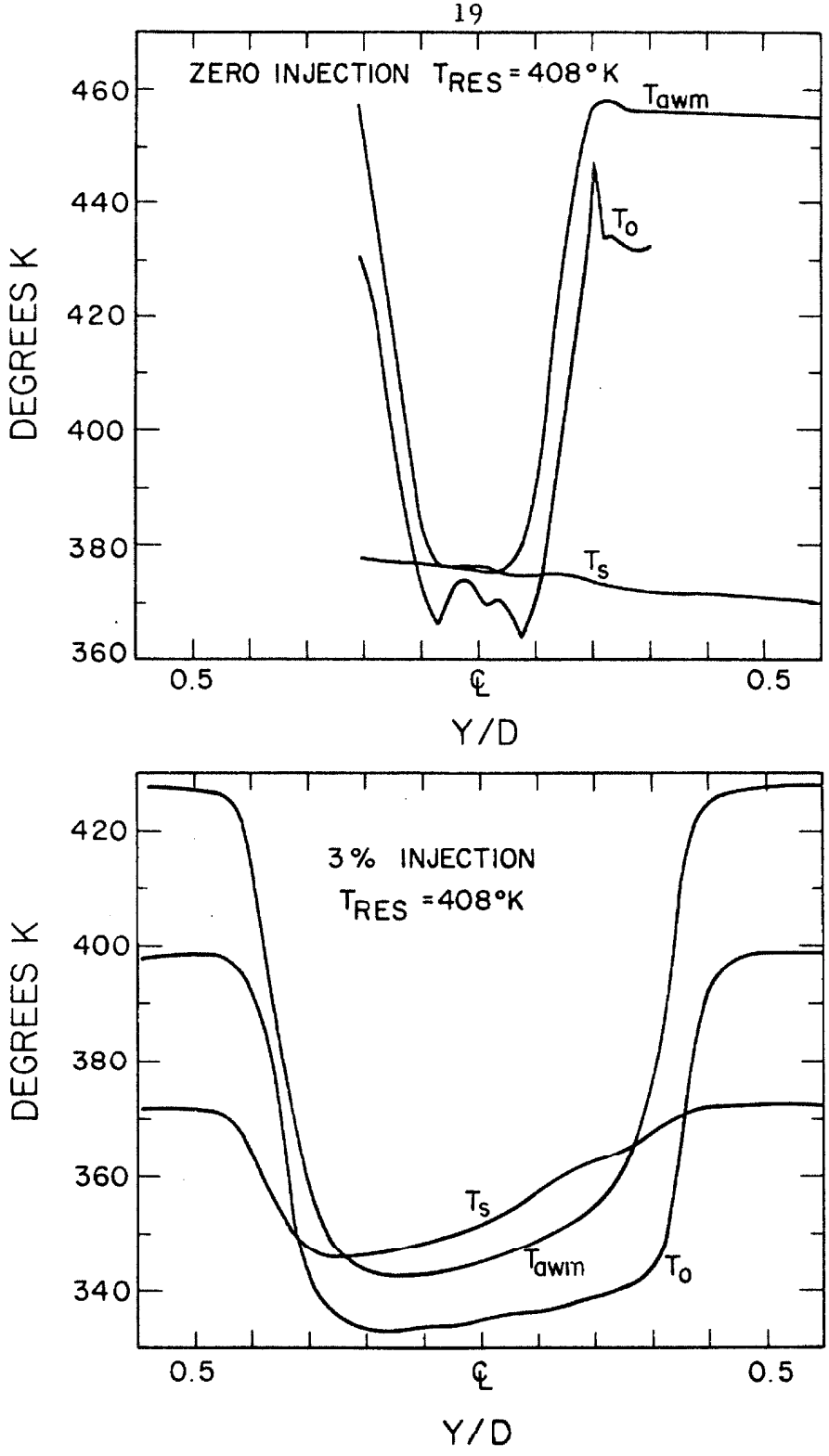


Fig. 7 Typical Support, Measured, and Total Temperature Across the Wake X/D = 1.5

the supports. The leads were insulated and attached to the needle and body of the probe with epoxy. On the body of the probe the leads were joined to glass insulated 28 gauge chromel-alumel thermocouple wire, which led to the outside of the tunnel where it was terminated with an ice cold junction and terminal strip. The hot wire was 1/10 mil platinum - 10 percent rhodium wire, soft-soldered to within .001" of the tips of the supports. The hot wires were anealed and calibrated as described by Dewey (12) . While calibrating the hot wires the thermocouple measuring system (amplifier, attenuator and digital voltmeter) was checked and found to be accurate to within $0.3^{o}C$.

The method of recording data used by Dewey was reliable and easy to use, but was in a form which required a great number of tedious calculations and point plottings to determine the measured Nusselt number and recovery temperature. Therefore, the recently acquired Datex recording equipment and IBM card punch were incorporated into an automated data recording system which would allow computer reduction of the recorded data. With the computer data reduction system it was possible to calculate the measured Nusselt number and recovery temperature for approximately 1000 data points per minute as compared with one point in 15 minutes by hand calculation.

The basic system is shown in block diagram form in Figure 8 and a complete description of the equipment is to be found in Appendix A. Basically the system is designed to vary the current through the

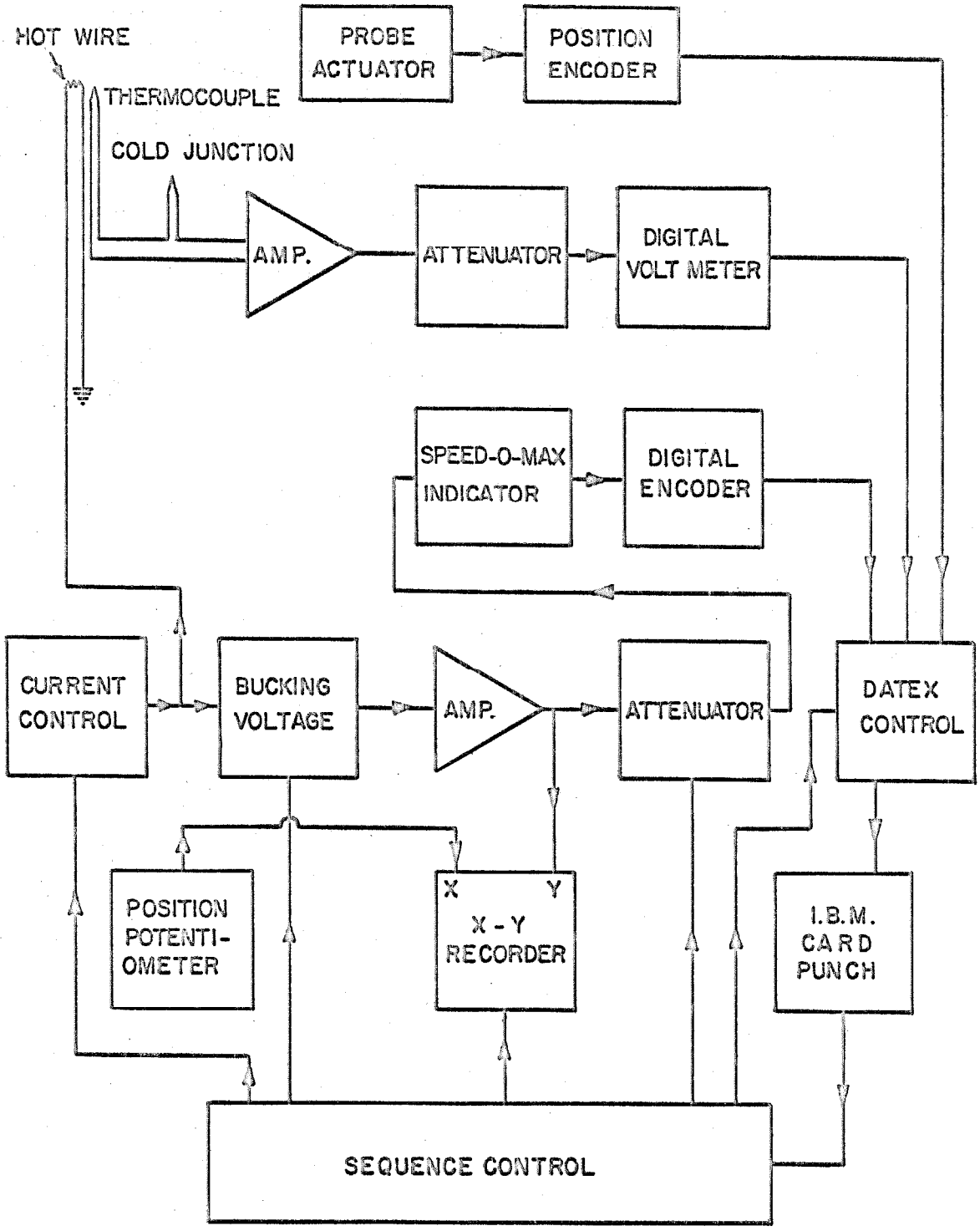


Fig. 8 Hot Wire Recording System Block Diagram

hot wire in five known discrete steps, to measure the voltage across the hot wire, and to record the five voltages, probe position, and support temperature on IBM cards. Since the voltage across the hot wire varies only slightly for a given current a bucking voltage for each current is used to cancel the major portion of the hot wire voltage. The differential voltage is then amplified and attenuated such that the indicator travels through most of its range during a survey. An encoder is attached to the indicator which sends a signal to the Datex control, where it is translated into digital form and then recorded on IBM cards. The sequence control is used to tie all the separate pieces of equipment together and sequence their operation.

It should be noted that this system differs from Dewey's in that it holds the probe stationary while sequencing through the five currents and therefore is more accurate in large gradients. As shown in Appendix A this system was capable of recording the data to sufficient precision to allow the calculation of resistance to $\pm 0.02$ ohms, which corresponds to about $\frac{1}{2}^{o}$ C.

# III. DATA REDUCTION

## III. 1 Pitot Pressure Measurements

In using the measured pitot pressure consideration was given to the effects of probe angle of attack, Reynolds number, probe size, and geometry. The maximum probe angle with respect to flow direction occurs in the zero injection case and is about $12^{o}$. In McCarthy's (11) investigation of the wake he calibrated the angle of attack sensitivity for a pitot probe and found that the correction was less than 1 percent for angles of attack up to $12^{o}$. Dewey (13) also made a study of the pitot pressure corrections by using several different probes to measure the same wake profile. The measured pressure profiles for all the probes were within 0. 7 percent.

Reynolds numbers outside the recirculation region and shear layer were on the order of 200 based on probe thickness and free stream conditions. Sherman (14) has investigated circular impact probes in this region of Reynolds and Mach number and shows the correction to be less than 1 percent for a $Re > 100$. Serious consideration needs to be given before making a quantitative analysis based on the pressures measured in the subsonic recirculation region, because there $Re < 10$. Sherman shows that the measured dynamic pressure in this subsonic low Reynolds number region is one to four times larger than the theoretical inviscid value. Mach numbers in this region should therefore be used only in a qualitative manner.

The effect of the probe on the flow within the subsonic recirculation region was considered, since the probe dimensions are large with respect to the size of the region. Dewey (13) has shown in his investigation that similar probes changed the base pressure by less than 1 percent and therefore it was concluded the effects were negligible. He also discusses why the displacement effects in the free shear layer could be ignored provided the probe thickness is less than 0.5 that of the shear layer thickness.

## III. 2 Static Pressure Measurements

In high velocity flows static pressure measurements are quite sensitive to angle of attack. McCarthy's (11) investigation showed a 2 percent correction for a $2^{o}$ angle of attack. For this reason only centerline pressure readings were used for actual data reduction. A survey across the wake was made to gain an idea of the uniformity of the static pressure with the results shown in Figure 9. No corrections were made for viscous interaction effects discussed by Behrens (15) because of the low Mach number along the wake centerline. The effect of moving the probe through a stagnation point in the recirculation region is not known and may cause some error in pressure measurement, or may shift the location of the stagnation point. It should be pointed out that the probe extended well into the shear layers at the rear most stagnation point. The two dimensionality of the flow geometry seems to be the primary factor in preventing a shift of the wake characteristics due to the presence of the probe.

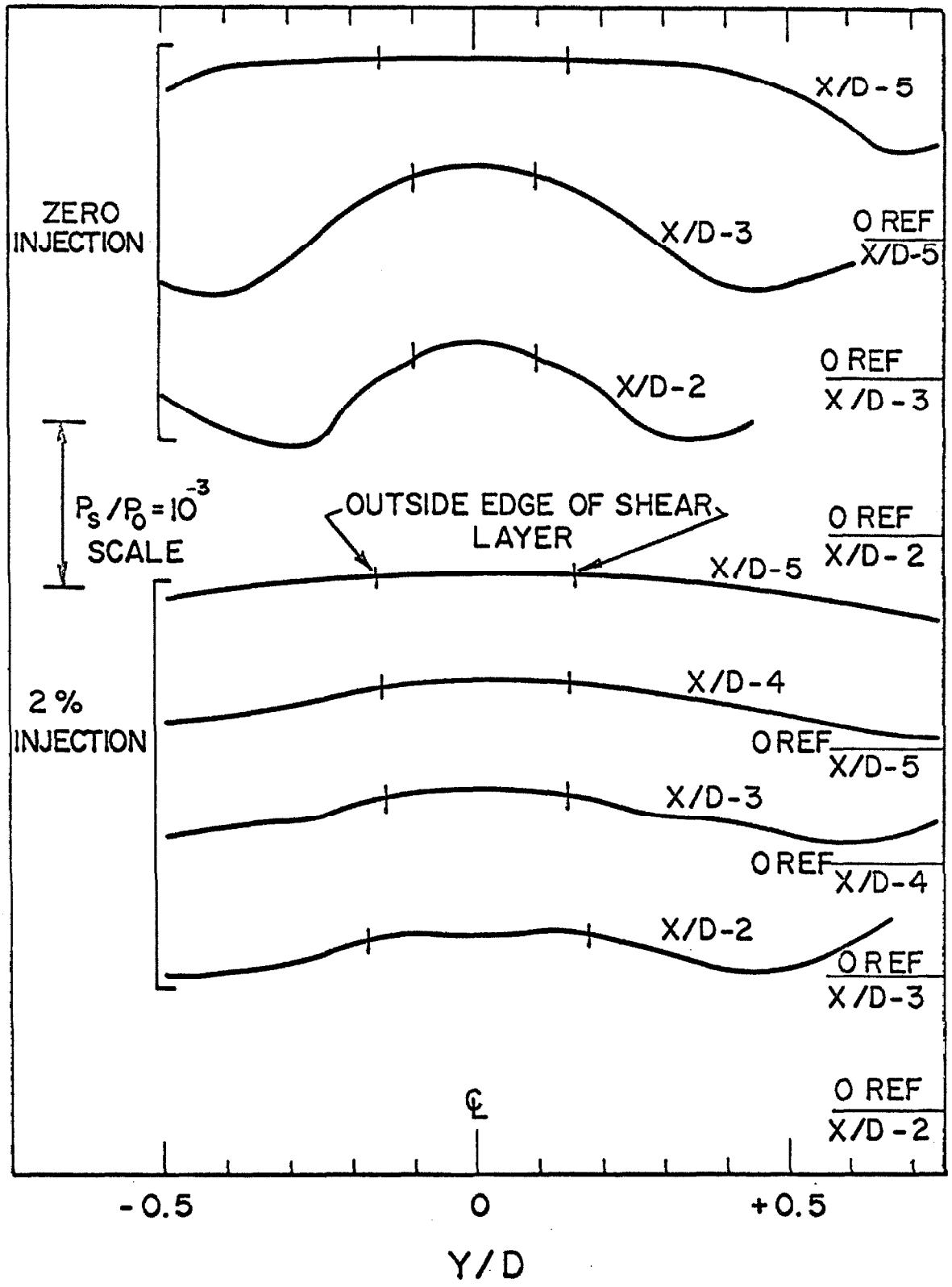


Fig. 9 Static Pressure Survey Across the Wake

Another indication that the interference effects were negligible was obtained by placing the pitot probe parallel and $\frac{1}{2}$" to the side of the rearward facing static probe and observing that both the pitot and static pressure increased by only 1 percent.

### III. 3 Hot Wire Measurements

Unlike pitot-static measurements, hot wire measurements are not readily reducible to flow field parameters except when the wire has been calibrated in a known flow. The calibration approach was not deemed satisfactory for this investigation because of the range of Mach number and the temperature gradient to which the probe would be subjected. A hot wire calibrated in a uniform flow has the end loss effect included in the calibration. If the probe supports are subjected to a large temperature gradient the equilibrium temperature is different from that for uniform flow and the change in end losses will invalidate a calibration made in uniform flow. It then becomes necessary to calculate the end losses as a function of the measured wire temperature and support temperature which was the problem solved by Dewey (12).

To use a finite length wire in determining recovery temperature, the effect of the support must be considered. Normally the support temperature is different from the mean wire temperature and the wire takes on a non-uniform temperature distribution with heat transfer both to the fluid and the supports. To calculate the corrected recovery temperature from the measured mean temperature, the

heat balance between the wire, the free stream and the supports must be known. Therefore, the Nusselt number ($Nu_m$) as well as the average wire temperature at zero current ($T_{awm}$) and the support temperature ($T_s$) must be obtained.

The support temperature was obtained by use of a thermocouple attached to one of the supports. Since the relationship between the hot wire resistance ($R_m$) and the electric heating $I^2R_m$ is linear for low overheats it is a simple matter to extrapolate to a zero current resistance ($R_{awm}$). Knowing $R_{awm}$ and the wire temperature coefficient $\alpha_r$ the temperature $T_{awm}$ can be calculated by:

$$T_{awm} = T_r + \frac{R_{awm} - R_r}{\alpha_r R_r} \tag{3.1}$$

The total temperature ($T_o$) can then be determined from

$$T_o = \frac{\psi_R}{\eta_*} \quad T_{awm} \tag{3.2}$$

where $\eta_*$ is the recovery factor for an infinite length wire and $\psi_R$ is the end loss correction factor. $\psi_R$ depends upon $\ell/d$, $(k_o/k_w)$, $T_s$ M and $Nu_m$ in relationships shown by Dewey (12). $Nu_m$ is defined by

$$Nu_m = \frac{d}{k_o} \quad \frac{q}{(T_{wm} - T_{awm})} = \frac{I^2 R_m}{\pi \ell k_o (T_{wm} - T_{awm})}$$

which becomes

$$Nu_m = \frac{a_r R_r}{\pi \ell k_o} \left[ \frac{R_m - R_{awm}}{I^2 R_m} \right]^{-1} \qquad (3.3)$$

by using the temperature-resistance relation.

Since $R_m$ is a linear function of $I^2 R_m$, then $\frac{R_m - R_{awm}}{I^2 R_m}$ is the slope of the $R_m$ versus $I^2 R_m$ curve. A computer program was used to reduce the measured data to a calculated curve of $R_m$ versus $I^2 R_m$ (see Appendix B). From the zero intercept and the slope of this curve the values of $T_{awm}$ and $Nu_m k_o$ were calculated and used as inputs for the end loss correction program developed by Dewey.

An attempt was then made to use the computer program developed by Dewey to calculate the flow field parameters from hot wire data and pitot pressure. For end loss corrections the program proved to be fairly satisfactory, but the calculation for Mach number was found to be non-convergent for $M < 1.5$. Dewey had pointed out the difficulty with using this program for $M > 4.0$, but it now appears advisable to rewrite the program using a variable other than Mach number. A discussion of this problem is to be found in Appendix B. Since time was not available to rewrite the program the end loss correction was computed using a Mach number calculated from pitot static pressure.

This approach was not completely satisfactory since it was not certain that the static pressure was constant across the wake. For data reduction purposes the static pressure was assumed constant to the outside edge of the shear layer. However, Figure 9 shows

that the measured static pressure is not constant across the wake. It should be remembered that this survey will have appreciable error induced by the moderate angle of attack off the wake centerline.

The computed values of $T_{awm}$ and $Nu_m$ showed smooth variation provided all the data was recorded with the same hot wire. Under these conditions the relative variation was less than 0.3 percent for $T_{awm}$ ($1^{\circ}K$) and less than 2 percent for $Nu_m$. Using different hot wires increased the maximum variation in repeatability to about 1.5 percent for $T_{awm}$ and 15 percent for $Nu_m$. This result indicates only fair absolute accuracy in the data and is difficult to explain, since the hot wire system was carefully calibrated and checked for shifts in bucking voltage and hot wire current. A check of the reliability of the data used in calculating the $R_m$ versus $I^2R_m$ curve was obtained by printing out the maximum deviation from the curve as part of the data output. This deviation seldom exceeded 0.02 ohms ($\frac{1}{3}^{\circ}C$). When the hot wire was not broken in shutting down the tunnel it was again calibrated. In the two cases checked $R_r$ was found to be within 0.5 percent of the previous calibrated value which could have accounted for about 0.7 percent of the shift in $T_{awm}$.

The usefulness of the data obtained would have been increased if centerline and outer wake reference values in the streamwise direction had been obtained using a single hot wire. Once the grid is established then the individual profiles could be shifted as

required to match the centerline and edge values and any traces with excessive shift could be re-run. While not increasing the absolute accuracy it would have increased the relative accuracy between the profiles for different injection rates and would have made analysis more reliable.

# VI. RESULTS

The results of injecting into the base region are most graphically demonstrated through the use of Schlieren photographs and pressure measurements. The lengthening of the base region and the disappearance of a strong wake shock are shown by the isoaxiometric pitot pressure profiles and Schlieren photographs in Figure 10 a-e. The shear layer no longer remains straight as it separates from the model but has a definite curvature, indicating an isentropic compression of the inviscid flow field outside the shear layer.

A qualitative idea of the centerline velocity distribution is obtained by superimposing the pitot and static pressures as shown in Figure 11. The low Reynolds number and reverse flow prevent quantitative determination of velocity, but the crossing of the pitot and static pressures give a good indication of the stagnation points. The double crossing of the pitot and static traces for 0.5 and 1.0 percent injection indicates that a small recirculation region exists

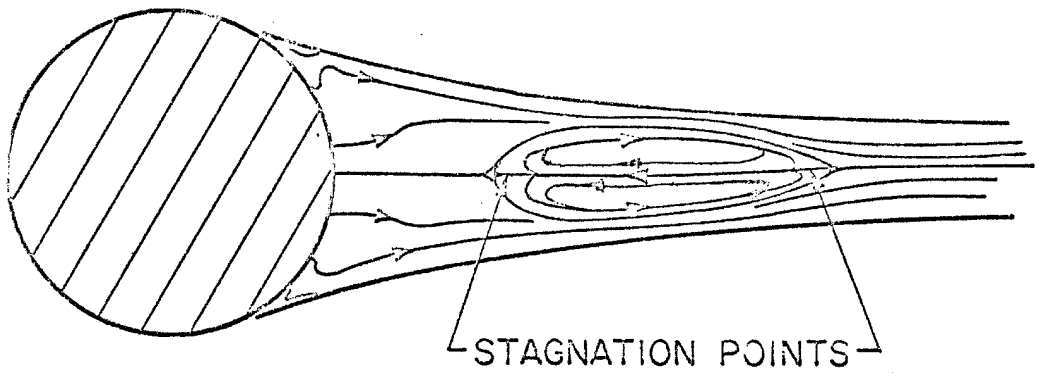


Fig. 12 Recirculation Region with Limited Injection

until the injection rate is increased to 1.5 percent. A suggestion of how this region might appear is shown in Figure 12.

The rear stagnation point for zero injection was checked using both a manometer and transducer to measure the pressures. These measurements placed the crossing of the pitot and static pressures at X/D = 1.6 as compared to X/D = 1.9 found by Dewey using hot wire measurements at a model Reynolds number of 22,000.

The forward movement of the separation point with increasing injection is shown in Figure 13 and helps to complete the picture of the changes occurring in the wake geometry. The movement of the separation point results from the increasing base pressure (Figure 14) associated with increasing injection rates.

The quantitative results of base injection are shown in Figures 15 and 16. The centerline static pressure distribution (Figure 15) shows a definite reduction in recompression in the neck region as the injection rate is increased. There is still a certain degree of recompression even when no recirculation is occurring, and this effect can be accounted for by the turning of the inviscid flow as it follows the shear layer. Figure 15 shows the normalized temperature distribution in the downstream direction. Only the uncorrected temperature $T_{awm}$ is presented because $T_o$ showed irregularities which are believed to have been induced by inaccuracies in the computer program (Appendix B-2). The difference between the measured temperature at the outer edge of the wake and the measured temperature at the base of the cylinder for each individual

injection rate was used as the normalization factor. Using this normalization procedure suppresses the portrayal of the cooling effects caused by injection, but shows that injection will increase the downstream distance required for the temperature to reach a uniform value.

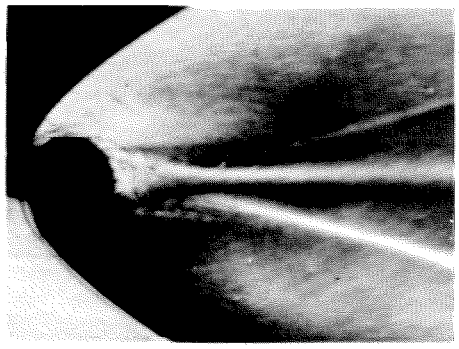

M = 6.08
$P_0$ = 80 psia
$T_{RES}$ = 408°K
0% INJECTION RATE

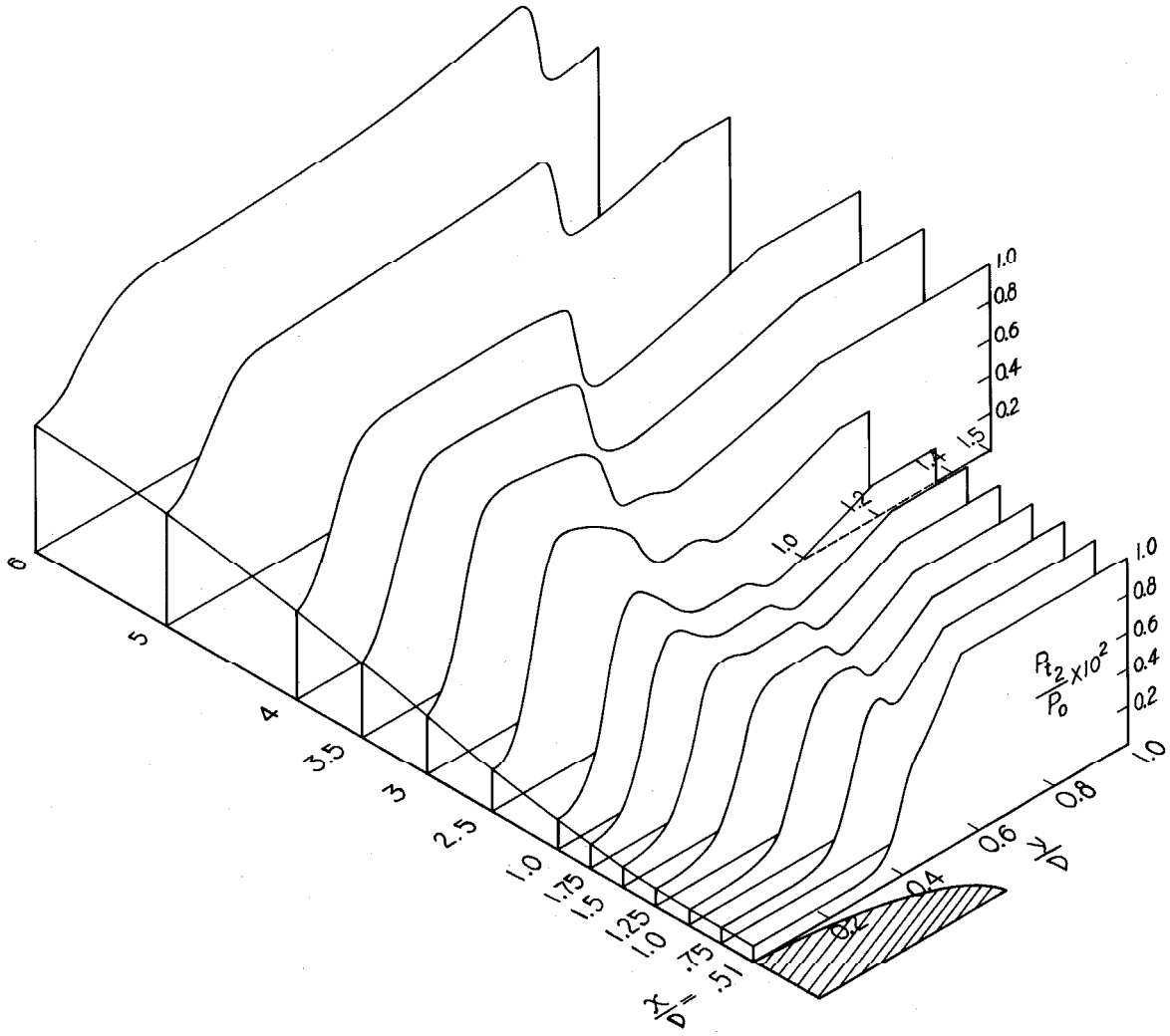


10a. Pitot Pressure Profiles and Schlieren Photograph

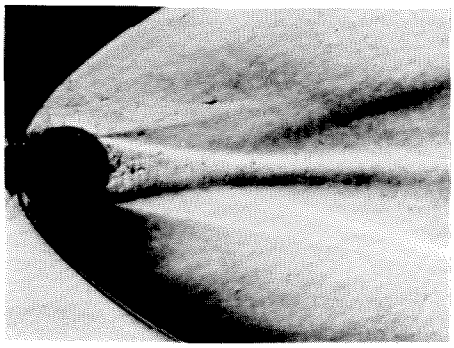

M = 6.08
$P_0$ = 80 psia
$T_{RES}$ = 408°K
1.0% INJECTION RATE

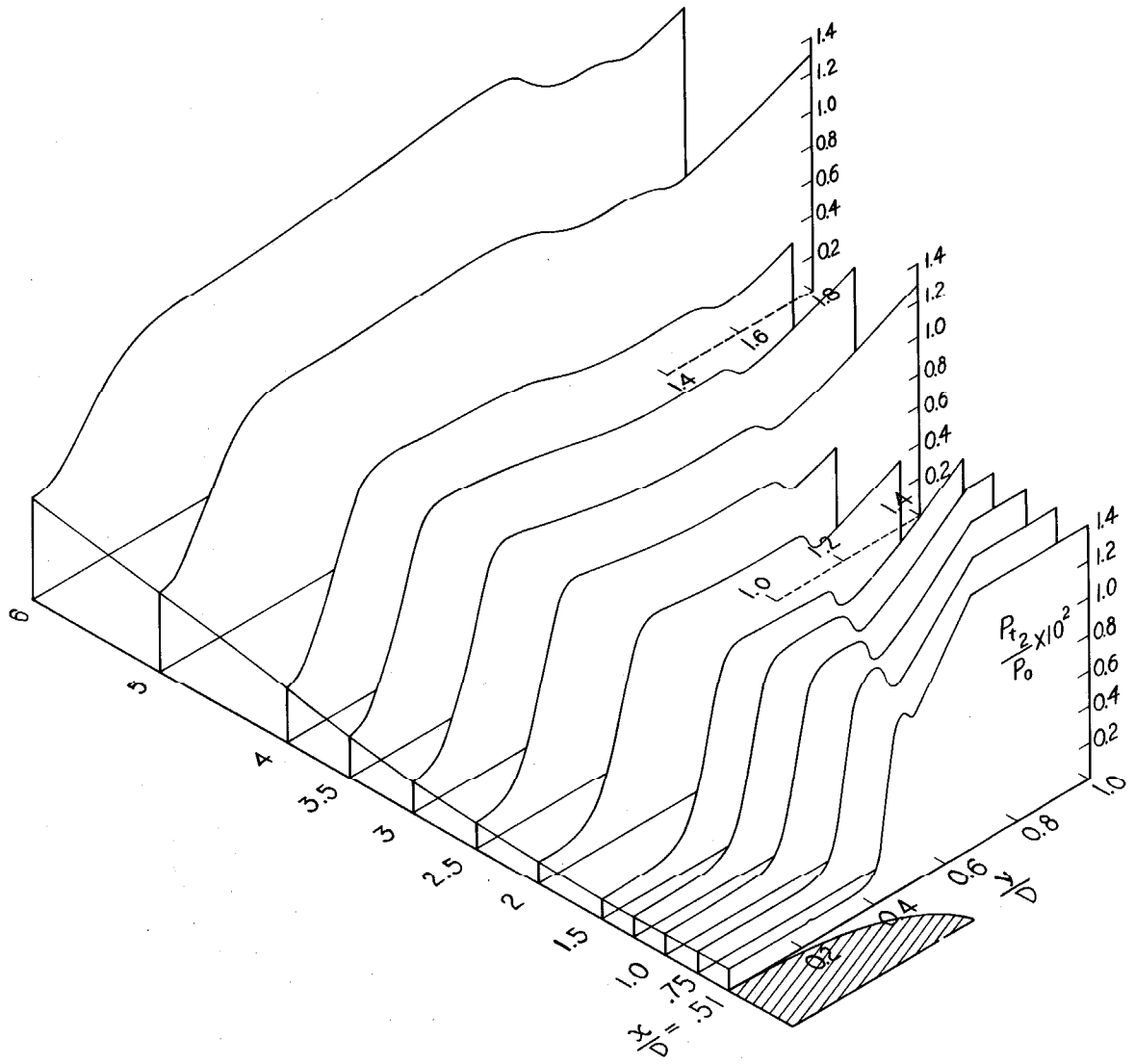


10b. Pitot Pressure Profiles and Schlieren Photograph

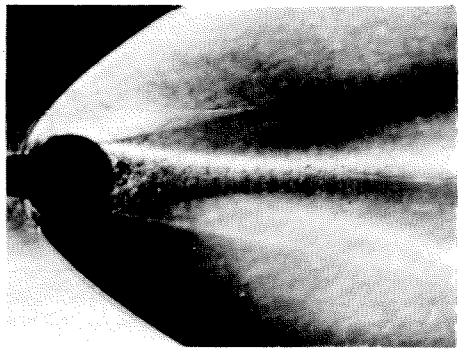

M = 6.08
$P_0$ = 80 psia
$T_{RES}$ = 408°K
1.5% INJECTION RATE

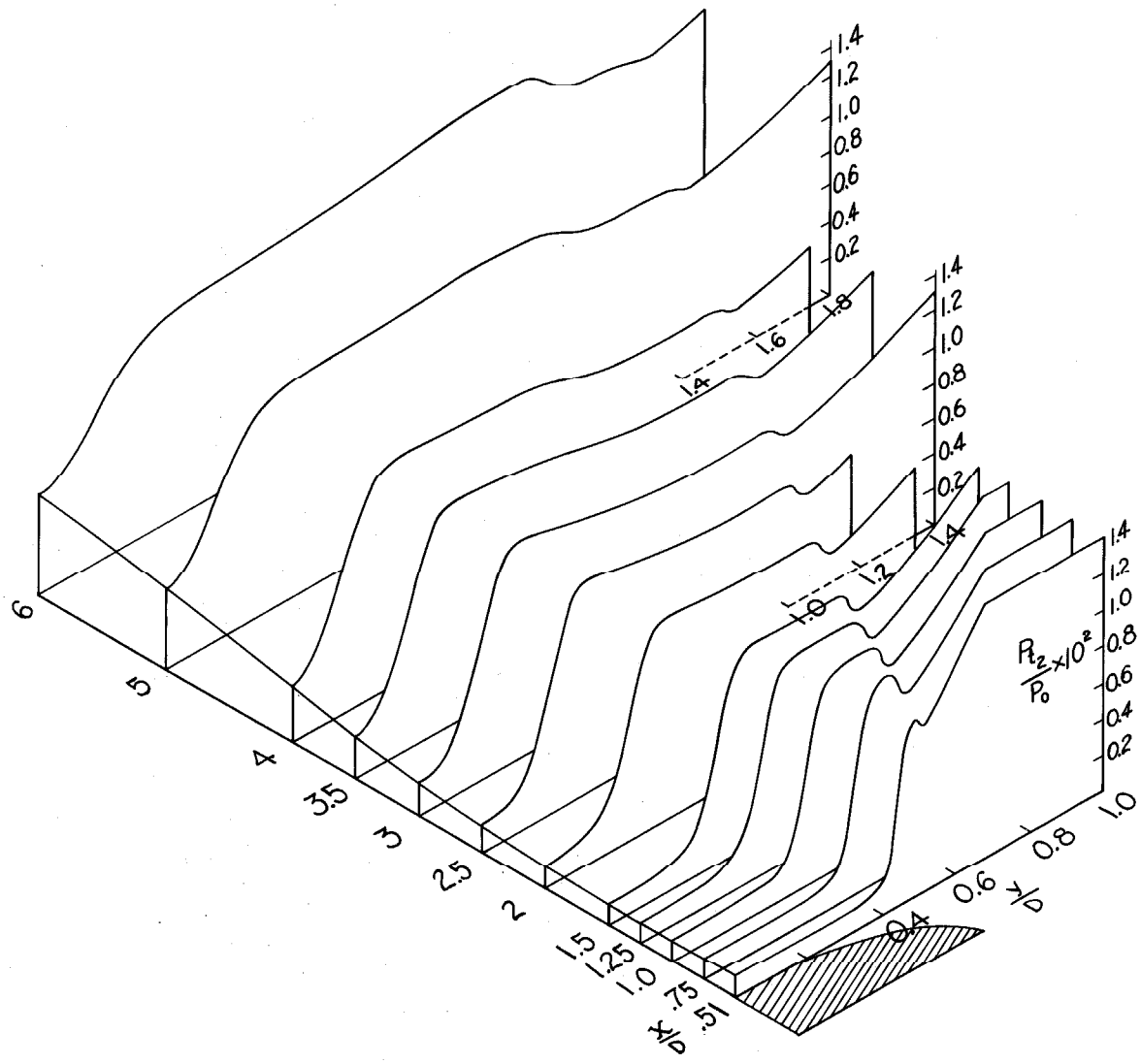


10c. Pitot Pressure Profiles and Schlieren Photograph

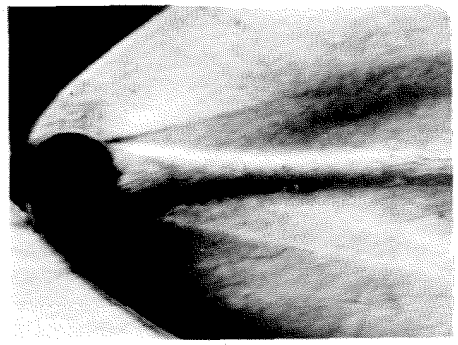

M = 6.08
$P_0$ = 80 psia
$T_{RES}$ = 408°K
2.0% INJECTION RATE

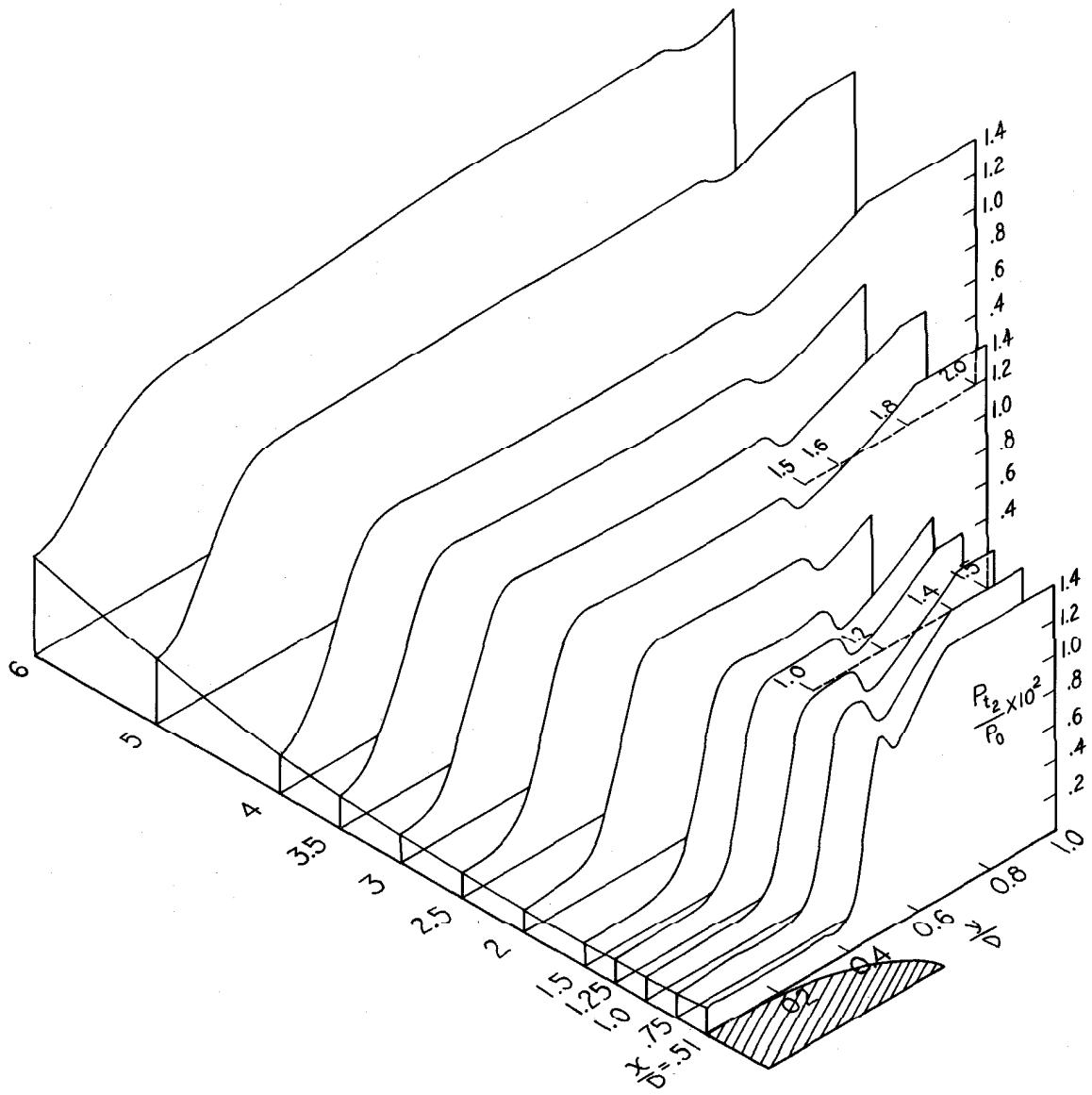


10d. Pitot Pressure Profiles and Schlieren Photograph

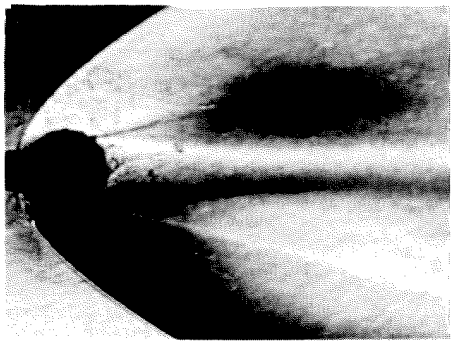

M = 6.08
$P_0$ = 80 psia
$T_{RES}$ = 408°K
3.0% INJECTION RATE

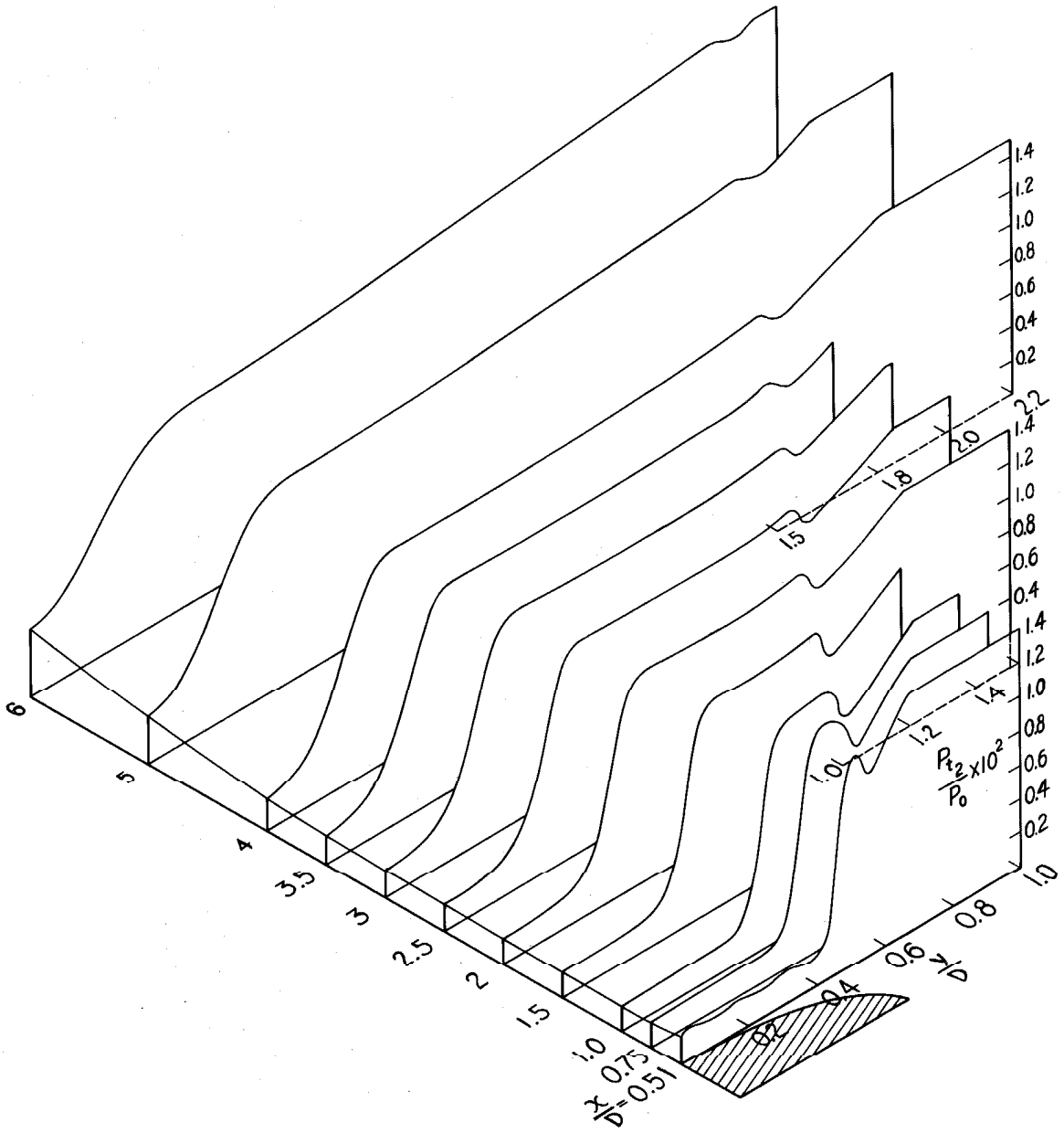


10e. Pitot Pressure Profiles and Schlieren Photograph

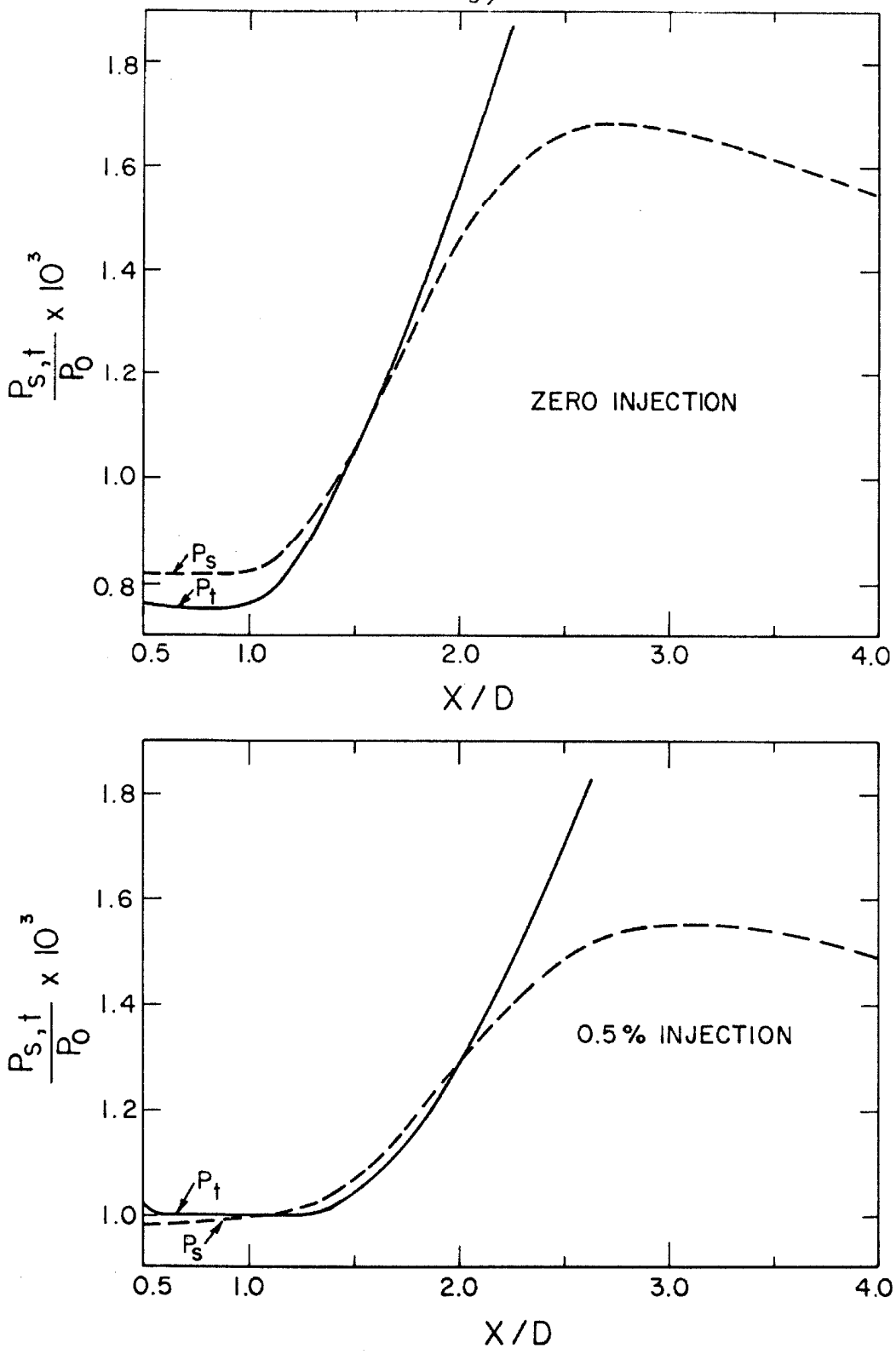


Fig. 11 Static and Pitot Pressure Survey, Wake Centerline

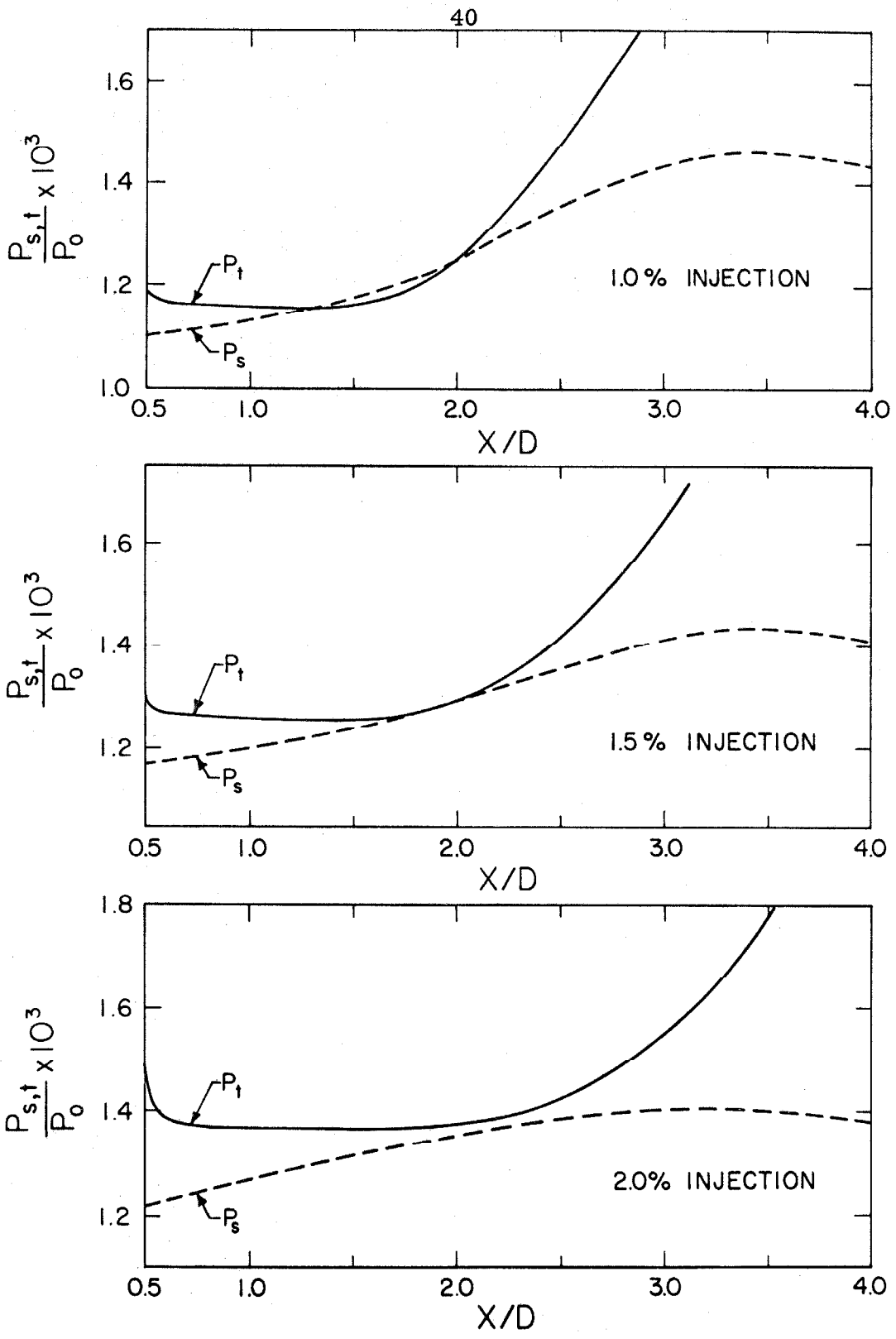


Fig. 11 Static and Pitot Pressure Survey, Wake Centerline

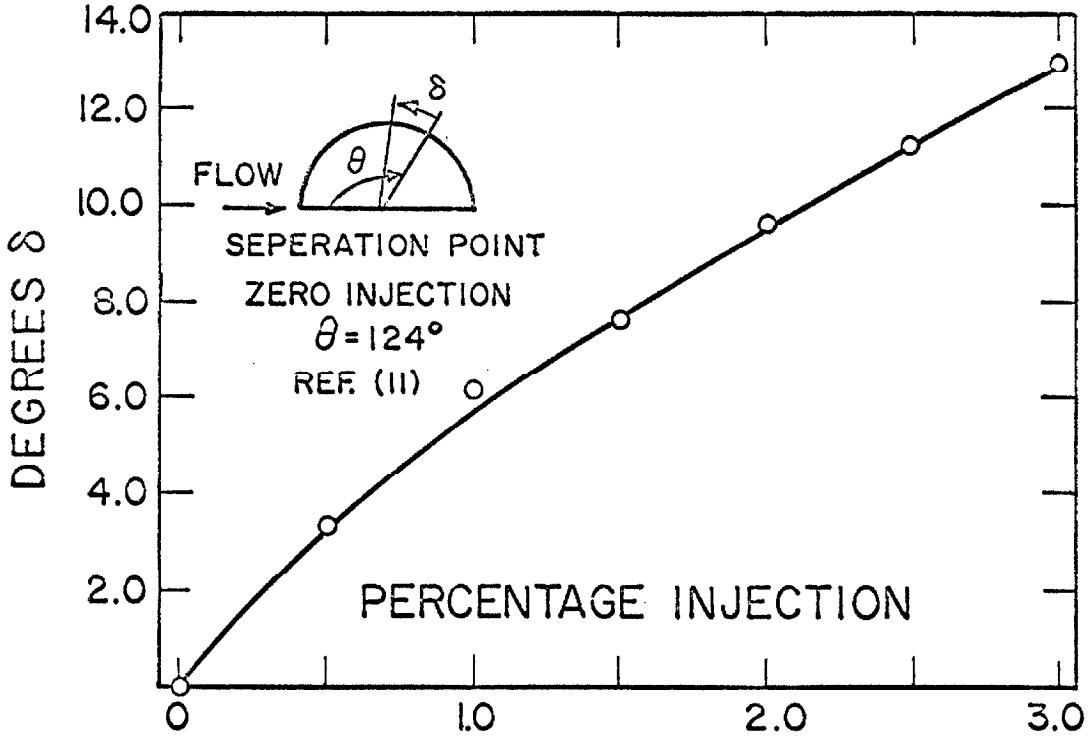


Fig. 13 Boundary Layer Separation Point Vs. Injection Rate

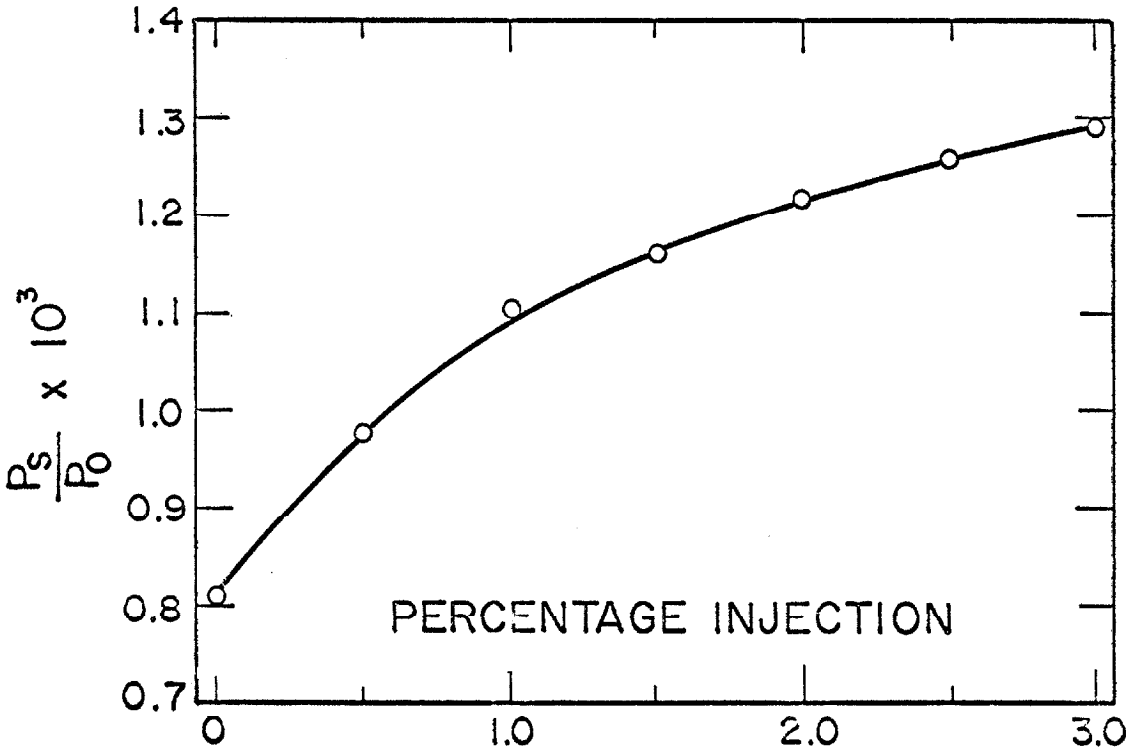


Fig. 14 Base Pressure Vs.Injection Rate

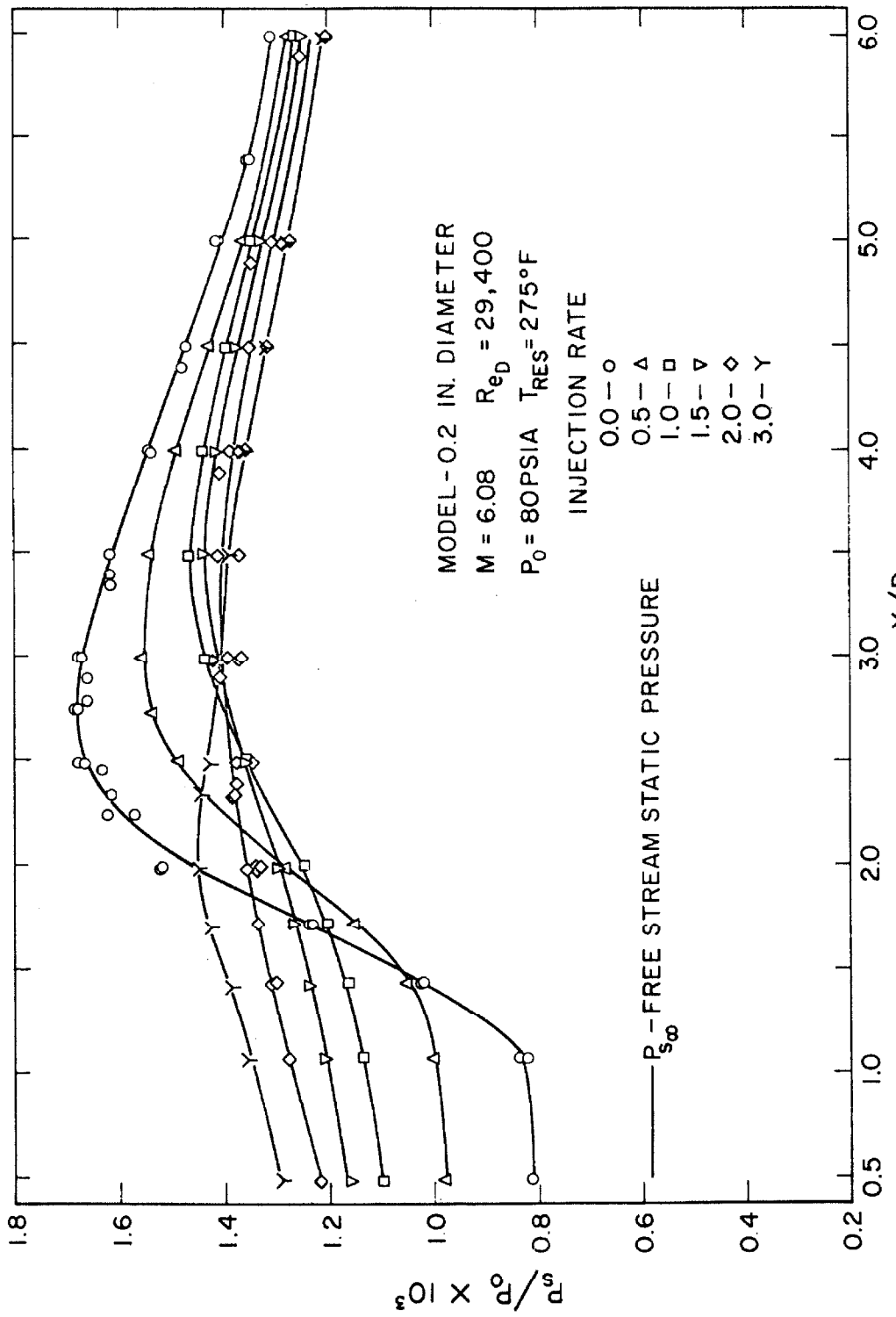


Fig. 15 Wake Centerline Static Pressure Vs. Injection Rate

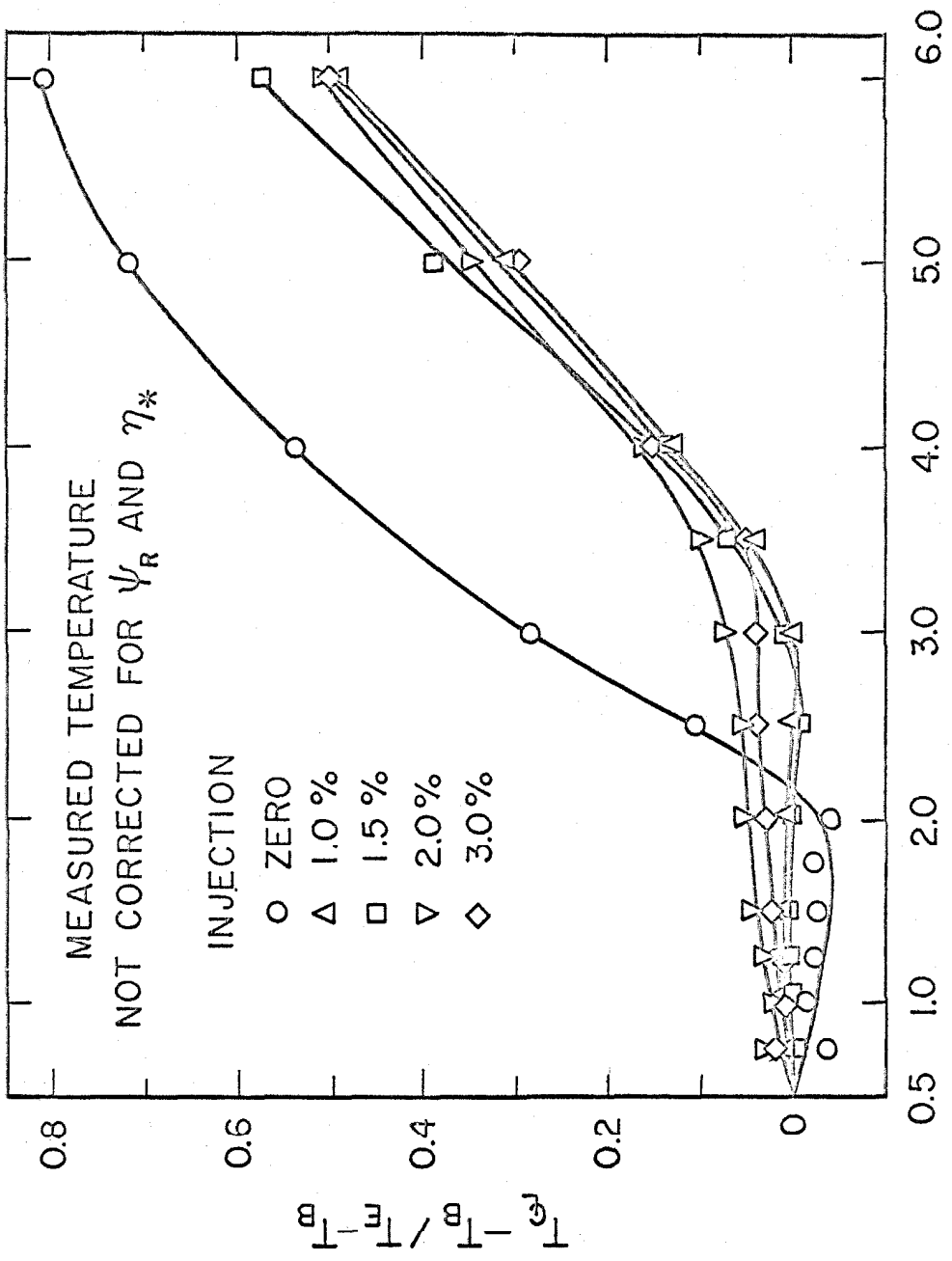


Fig. 16 Wake Centerline Measured Temperature Vs. Injection Rate

# V. SUGGESTIONS FOR FURTHER STUDY

The effects of small injection rates on the near wake are quite pronounced and the investigation could be continued in many different directions. The study could be carried on further downstream, with particular attention given to the effects of injection on laminar-turbulent transition and the distance required for the effects of injection on temperature to die out. Another avenue of investigation would be to vary the Reynolds number. This was done on some preliminary test and indicated that the rate of injection required to give the same wake geometry increases as the Reynolds number is decreased, as expected from laminar mass entrainment considerations. Changing the temperature of the injected gas could be attempted, however, experience with the present model indicates that this would tend to change the model temperature because of the ratio of model thermal conductivity to that of air. Changing the injected gas to helium or argon would allow for determination of the mixing process and transition by means of concentration measurements.

There is still need for improvement in the computer program for hot wire data reduction. This will require the selection of more suitable variables within the program to make it less sensitive to the accuracy of the measured data. Consideration should be given to using the Stanton number and dividing the program up into subregions as discussed in Appendix B-2. The temperature of both supports needs to be checked and if there is a difference in

temperature further improvement in the recording system and computer program is possible.

# REFERENCES


1. Chapman, D. R., Base Pressure at Supersonic Velocities, Ph. D. Thesis, California Institute of Technology, Pasadena, (1948).

2. Chapman, D. R., Laminar Mixing of a Compressible Fluid, NACA Report 958, (1950).

3. Chapman, D. R., An Analysis of Base Pressure at Supersonic Velocities and Comparison with Experiment, NACA Report 1051 (1951). (Supersedes NACA TN 2137 (1950)).

4. Chapman, D. R., Kuehn, D. M. and Larson, H. K., Investigation of Separated Flows in Supersonic and Subsonic Streams with Emphasis on the Effect of Transition, NACA Report 1356, (1958).

5. Lees, L. and Hromas, L., Turbulent Diffusion in the Wake of a Blunt-Nosed Body at Hypersonic Speeds, Aerodynamics Department Report 50, Space Technology Laboratories, Inc., July (1961). Also, Journal of the Aerospace Sciences, Vol. 24, No. 8, pp. 976-993, August (1962).

6. Lees, L., Hypersonic Wakes and Trails, AIAA Journal, Vol. 2, No. 3, pp. 417-428, January (1964).

7. Kubota, T., Laminar Wake with Streamwise Pressure Gradient, GALCIT Internal Memo. No. 9, April (1962).

8. Mohlenhoff, W., Experimental Study of Helium Diffusion in the Wake of a Circular Cylinder at M = 5.8, GALCIT Hypersonic Research Project, Memo No. 54, May 20 (1960).

9. Kingsland, L., Jr., Experimental Study of Helium and Argon Diffusion in the Wake of a Circular Cylinder at M = 5.8, GALCIT Hypersonic Research Project, Memo. No. 60, June 1, (1961).

10. Demetriades, A., Some Hot-Wire Anemometer Measurements in a Hypersonic Wake, Proceedings of the 1961 Heat Transfer and Fluid Mechanics Institute, Stanford University Press, (1961).

11. McCarthy, J. F., Jr., Hypersonic Wakes, GALCIT Hypersonic Research Project, Memo. No. 67, July (1962).

12. Dewey, C. F., Jr., Hot-Wire Measurements in Low Reynolds Number Hypersonic Flows, GALCIT Hypersonic Research Project, Memo. No. 63, September (1961). (Computer Program not included). Ph. D. Thesis (Part I), California Institute of Technology, Pasadena, California (1963). (Includes Computer Program and several corrections to first publication).

13. Dewey, C. F., Measurements in Highly Dissipative Regions of Hypersonic Flows, Part II. The Near Wake of a Blunt Body at Hypersonic Speeds. Ph. D. Thesis (Part II), California Institute of Technology, Pasadena, California (1963).

14. Sherman, F. S., New Experiments on Impact-Pressure Interpretation in Supersonic and Subsonic Rarefied Air Streams, NACA TN 2995 (1953).

15. Behrens, W., Viscous Interaction Effects on a Static Pressure Probe at M = 6, AIAA Journal, Vol. 1, No. 12, pp. 2864-2866, December (1963).

16. Sherman, F. S., A Survey of Experimental Results and Methods for the Transition Regime of Rarefied Gas Dynamics, International Symposium on Rarefied Gas Dynamics, Vol. II, Academic Press, New York(1963).

17. Stalder, J. R., Goodwin, G., and Creager, M. O., A Comparison of Theory and Experiment for High-Speed Free-Molecule Flow, NACA Report 1032, (1951).

# APPENDIX A

## AUTOMATED HOT WIRE RECORDING SYSTEM

In determining the Nusselt number and recovery temperature it is necessary to measure the hot wire resistance using several different heating currents. The heating currents are kept small to simplify data reduction, but these small currents produce only small changes in hot wire resistance. In measuring this resistance change the ideal solution would be to use a bridge circuit with automatic balance and digital readout. Lacking a self-balancing bridge the system was designed to use a null balancing potentiometer to measure voltage variation. Knowing the voltage across, and the current through the hot wire, the resistance could be calculated. A bucking voltage was used to cancel most of the voltage across the hot wire for each current. Therefore, only the change in differential voltage was measured, and this procedure increased the accuracy of the recorded data by an order of magnitude.

A modified schematic of the hot wire system showing only the basic features of the circuit is shown in Figure 17. This circuit required that the bucking voltages and currents remain very stable; therefore low temperature coefficient resistors were used in all critical circuits. In addition the equipment was turned on several hours before use to allow for stabilization of the component parts.

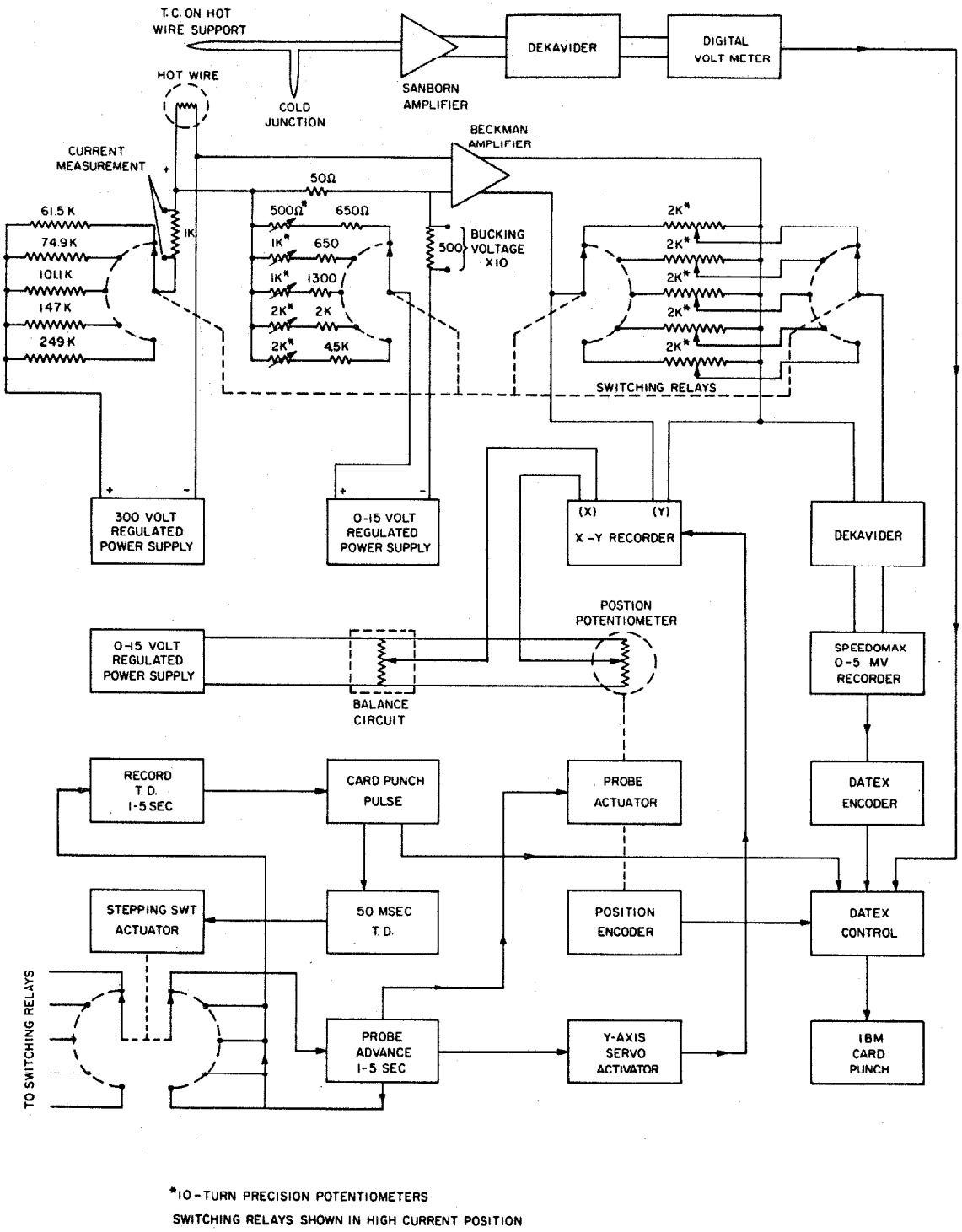


*10-TURN PRECISION POTENTIOMETERS

SWITCHING RELAYS SHOWN IN HIGH CURRENT POSITION

Fig. 17 Simplified Schematic for Hot Wire Recording System

The current is regulated by five limiting resistors which limit the current from a constant voltage power supply. The hot wire current is measured by using the digital voltmeter which reads the voltage across a 1000 ohm resistor placed in series with the hot wire. The current is effectively constant, since the variation of hot wire resistance is less than $10^{-4}$ times the total resistance; provided of cource that the power supply and limiting resistors are stable. Measurement of current variation showed it to be less than 0.05 percent over a period of several hours.

The voltage differential between the hot wire and bucking voltage was amplified with a Beckman Amplifier. Since the input impedance of the amplifier exceeded 100 megohms there is essentially zero current flow through the hot wire voltage measuring circuit to ground. The bucking voltage was obtained by generating a current flow through a 50 ohm resistor in series with the amplifier input using a stabilized, isolated power supply. Because current does not flow in the hot wire voltage measuring circuit the voltage drop across the 50 ohm resistor was a function only of the current flow in the bucking voltage circuit. The current is controlled by one of five variable limiting resistors and the setting of the power supply voltage. The bucking voltage is measured by reading the voltage across a 500 ohm resistor in series with the bucking voltage circuit, and dividing the results by ten. Variation of the bucking voltage was less than .01 percent over a period of several hours.

The differential between hot wire and bucking voltage was amplified by a factor of 100 and then the output was attenuated by one of five potentiometers used as voltage dividers. Separate voltage dividers were used because the voltage differential varied with hot wire current. The output was further attenuated using a Dekavider to match the input requirements of the Speedomax Null balancing potentiometer. The voltage differential measured by the Speedomax moved a recording hand on the indicator which was coupled to a digital encorder. The output of the encorder was translated by the Datex control unit and was recorded on an IBM card with the card punch. The error attributed to the amplifier and attenuators combined is less than 0.03 percent. The accuracy of the Speedomax recorder and encorder, while within specification, amounted to $\pm$ 0.4 percent full scale which was not negligible. It is now obvious why the system was designed to use the Speedomax to record differential voltages rather than the total voltage across the hot wire.

A plot of the differential voltage output versus position was made on an X - Y plotter for the high current trace only, and provided a means of monitoring the hot wire measurements. The high current trace was used because it gave the best indication of variation in the flow field. The position of the probe was measured with a digital encorder connected to the probe traversing mechanism. The output of the encorder was fed to the Datex translator and then punched on the IBM card with the card punch. This system was accurate to

$\pm$ .002 in. provided the probe movement was always in the same direction. The position signal for the X - Y recorder was obtained by using a 40 turn potentiometer as a voltage divider in a manner similar to that for pressure measurements.

Needle support temperature was measured with a chromel-alumel thermocouple terminated with an ice cold junction. The output signal was amplified and attenuated such that the voltage output corresponded to temperature in $^{o}$C (1.00 volt = 100$^{o}$C). The voltage was read by the digital voltmeter and recorded on the IBM cards using the Datex control unit and the card punch. The thermocouple output is not perfectly linear with temperature, and therefore the amplifier zero offset in conjunction with the attenuator was used to linearize the curve about the average operating temperature.

A sequence control ties all the circuits together and sequences their recording in the proper order. A stepping switch is used to sequence the proper current, bucking voltage and attenuation factor. Time delays allow for the proper nulling of recording equipment. The sequence of operations for one cycle is as follows:

1. Advance probe, select highest current, bucking voltage and attenuator setting.
2. Activate Y servo on X - Y recorder.
3. Time delay to allow for nulling of Speedomax recorder.
4. Command to print position and recorder reading, de-activate Y servo on X - Y recorder.
5. Select lower current, bucking voltage and attenuator setting.
6. Time delay to allow for nulling of Speedomax recorder.

7. Print recorder reading.
8. Repeat Steps 5, 6 and 7 for two lower currents.
9. Select lowest current bucking voltage and attenuator setting.
10. Repeat Step 6.
11. Print recorder reading, needle support temperature, card identifying data, and advance to new IBM card.
12. Repeat cycle starting with Step 1.

This cycle, which is repeated as often as desired as the probe advances across the wake, takes approximately 10 - 15 seconds. The distance between data points is selected by varying the operating time and speed of the probe traversing mechanism.

# APPENDIX B

## DATA REDUCTION PROGRAM

### B. 1 Preliminary Data Reduction

The purpose of the preliminary program is to determine $T_{awm}$ and $Nu_m k_o$ from input data generated by the hot wire recording system. This was done by first calculating $R_m$ and $I^2 R_m$ for each of the five currents by:

$$R_{m_j} = \frac{E_{w_j}}{I_j} \qquad \left[I^2 R_m\right]_j = E_{w_j} I_j \qquad j = 1 - 5$$

The voltage across the hot wire ($E_w$) was not measured directly but can be obtained from the measured voltage $E_m$ by

$$(E_w + E_{lead} - E_{bucking})\ (\text{amp.})\ (\text{atten.})\ (\text{scale factor}) = E_m$$

The bucking voltage and lead voltage drop were measured at convenient intervals and their difference was read into the program as constants, CO(j + 15). The product of the amplification, attenuation and scale factors was likewise read in as constants, CO(j + 20).

A least squares fit was calculated to give the best straight line through the data points. The zero intercept and slope of the line were then used to calculate $T_{awm}$ and $Nu_m k_o$ using the calculations shown in Equations (3. 1) and (3. 3). In addition a check of the input

data was made by checking for the maximum difference between the straight line and the data points. Reference to the following program listing and computer program will give a more detailed understanding of the exact computations.

Program listings

INPUT DATA

$Q_1$ = Probe position (in.) $Q_1 = T_s(^oC)$

$A_j = E_m$

CORNO = a sequenced card number for identification

INPUT CONSTANTS

CO(1) = wake centerline (in.) CO(2) = $R_r$ CO(3) = $a_r$

CO(6) = $\ell$ PCI = percent injection XD = X/D

ID = Hot wire no. $CO(j + 10) = \left[(\text{amp.})\ (\text{atten.})\ (\text{scale factor})\right]_j^{-1}$

$CO(j + 15) = \left[E_{bucking} - E_{lead}\right]_j$ $CO(j + 20) = I_j$

OUTPUT DATA

$z_1 = Y/D$ $z_2 = R_m$ $z_3$ = slope

$z_4 = T_{awm}$ $z_5 = Nu_m k_o$ $z_6 = T_s(k^o)$

DIFMAX = Maximum deviation of $R_m$ from calculated straight line through data points.

# PRIMARY DATA REDUCTION PROGRAM*

```
20 READ (5,500)Q1, (A(J),J=1, 5), Q7,CORNO
   DO 30 J = 1, 5
   B(J) = A(J) * CO(J+10)
   C(J) = B(J) + CO(J+15)
   D(J) = C(J) / CO(J+20)
   E(J) = C(J) * CO(J+20)
30 CONTINUE
   CALL LSTSQ(E,D,X2,X1)
   DO 35 J = 1,5
   DEVAL = X2*E(J)+X1
   DIF(J) = D(J) - DEVAL
35 CONTINUE
   DIFMAX = DIF(1)
   DO 36 J = 2,5
   IF(ABS(DIFMAX) .GT. ABS(DIF(J))) GO TO 36
   DIFMAX = DIF(J)
36 CONTINUE
   Z1 = (Q1 - CO(1)) * 5.0
   Z2 = X1
   Z3 = X2
   Z4 = 273.2 + (Z2-CO(2)) / (CO(2)*CO(3))
   Z5 = CO(2) * CO(3) / (3.1415926 5*CO(6) *Z3)
   Z6 = Q7 + 273.2
   WRITE (6,515) PCI,XD,Z1,Z2,Z3,Z4,Z5,Z6,
   ID,CORNO  DIFMAX
   PUNCH 600,    PCI, XD, Z1, Z2, Z3, Z4, Z5, Z6 ID,
   GO TO 20

   SUBROUTINE LSTSQ(X,Y,A,B)
COMPUTE THE SLOPE OF A LEAST SQUARES FIT THROUGH PTS X, Y
A IS THE SLOPE AND B IS THE Y INTERCEPT
   DIMENSION X(5), Y(5), C(5)
   DO 10 I = 1, 5
   C(I) = 0.0
10 CONTINUE
   DO 20 I = 1, 5
   C(1) = C(1) + X(I)
   C(2) = C(2) + X(I)**2
   C(3) = C(3) + Y(I)
   C(4) = C(4) + X(I)*Y(I)
20 CONTINUE
   B = (C(4) - C(3)*C(2) / C(1)) / (C(1)-5.0*C(2) / C(1))
   A = (C(3) - 5.0*B) / C(1)
   RETURN
```

* Note all storage, accounting and format statements have been deleted.

## B. 2 Final Data Reduction Program

The purpose of the final data reduction program is to compute the hot wire end loss corrections, recovery factor, and flow field variables. Dewey's (12) program was converted to Fortran IV which is now used by the computing center. The input statement and support temperature calculation were altered to accept the output data from the preliminary program including the measured support temperature. After each change the program was checked against Dewey's M = 1.63 test case and found to be slowly convergent. The program was then used to reduce the data measured along the wake centerline. These calculations did not converge or else the calculated value went to one of the Mach number limits in the program. Changes were then made in the way M and $\psi_N$ were calculated and marginal results were obtained.

The difficulty with the original Mach number calculation resulted from the Mach number dependence of $Re_o$ for $M < 3.5$. In Dewey's program $Re_o$ was used to calculate F 17.

$$F\ 17 = \frac{Re_o\ M_o}{d\ P_{t_2}} \sqrt{\frac{\gamma + 1}{2}\ R\ T_o} \qquad \text{(B-1)}$$

Mach number was then obtained from $(F\ 17)^2$ by an iterative procedure using one of the following equations.

For $M < 1$

$$\left(\frac{\gamma+1}{2} M^2\right)\left(1+\frac{\gamma+1}{2} M^2\right)^{-\left(\frac{\gamma+1}{\gamma-1}\right)} = (F\ 17)^2$$

and for $M > 1$ (B-2)

$$\left(1+\frac{\gamma-1}{2} M^2\right)\left(\frac{\gamma+1}{2} M^2\right)^{-\left(\frac{\gamma+1}{\gamma-1}\right)}\left(\frac{2\ M^2-(\gamma-1)}{+1}\right)^{\frac{2}{\gamma-1}} = (F\ 17)^2$$

Dewey recognized that this calculation was unsatisfactory for $M > 4.0$. The reason for this can be seen in Figure 18, which snows that M is very sensitive to changes in $(F\ 17)^2$ for large M. What was not recognized, however, was that the computer program used in determining Mach Number was not convergent because of the repeated calculation of $Re_o$ which was itself Mach number dependent for $M < 3.5$.

$Nu_o$ and M are used to calculate $Re_o$ in the computer subroutine NUOREO. For the first trial solution M is arbitrarily assumed and in subsequent iterations it is obtained by solving equation (B-2) for M (subroutine MF 22). A typical example of divergence can be seen in Figure 18 which shows the function $(F\ 17)^2$ as calculated from both equations (B-1) and (B-2). Assume that all the measured values are correct, that the end loss corrections have been made and the correct value for $M = 1.2$. If the initial guess for M is $M = 1.3$, then $Re_o$ calculated by NUOREO would be too large and $(F\ 17)^2$ calculated by equation (B-1) would be too large, point 1. Then M calculated by MF 22 equation (B-2) would be too small, point 2. This would lead to a much lower value of $Re_o$ in the succeeding calculation of NUOREO

with consequent large reduction in $(F\ 17)^2$, point 3. The calculation would continue to diverge as shown by the arrows in the figure. It is apparent that whenever $\left|(1/Re_o)^2 \{d(Re_o)^2/dM\}\right| > \left|(1/F\ 17)^2 d(F\ 17)^2/dM\right|$ where $(F\ 17)^2$ is calculated by equation (B-2) then the Mach number calculation will diverge. To find the region of convergence the computer subroutines NUOREO (calculation of $Re_o(M, Nu_o)$) and MF 22 (calculations of equations (B-2) ) were evaluated and differentiated to give the results shown in Figure 19. For $M < 1.5$ the program is non-convergent. When the initial guess for $M < 1$ both derivatives of $(F\ 17)^2$ and $Re_o^2$ are positive and M is quickly iterated to the program limit of $M = 0.2$ or $M = 1.0$. When $1.0 < M < 1.5$ the derivatives of $(F\ 17)^2$ and $Re_o^2$ are of opposite sign and the iteration diverges in an

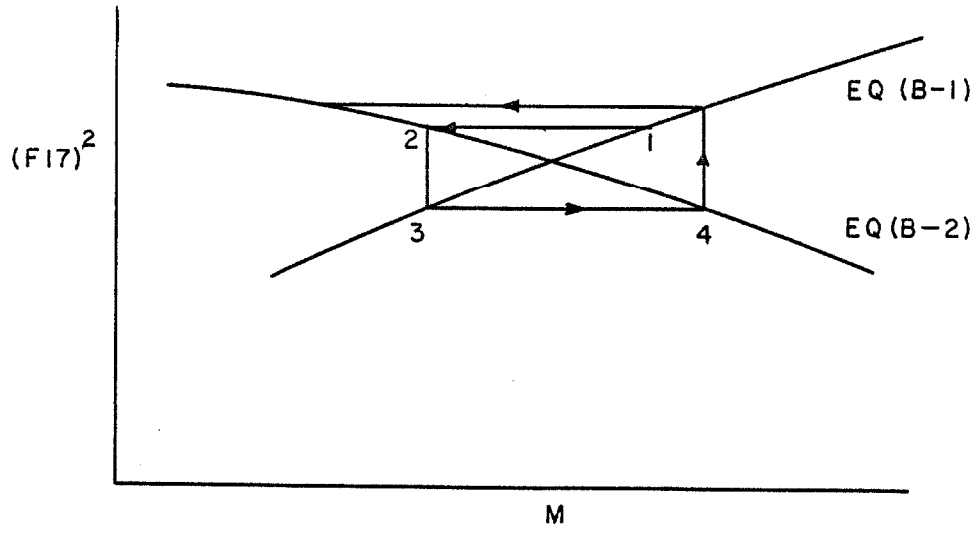


Fig. 18 Typical Values of Calculated Mach Number $1.0 < M < 1.5$

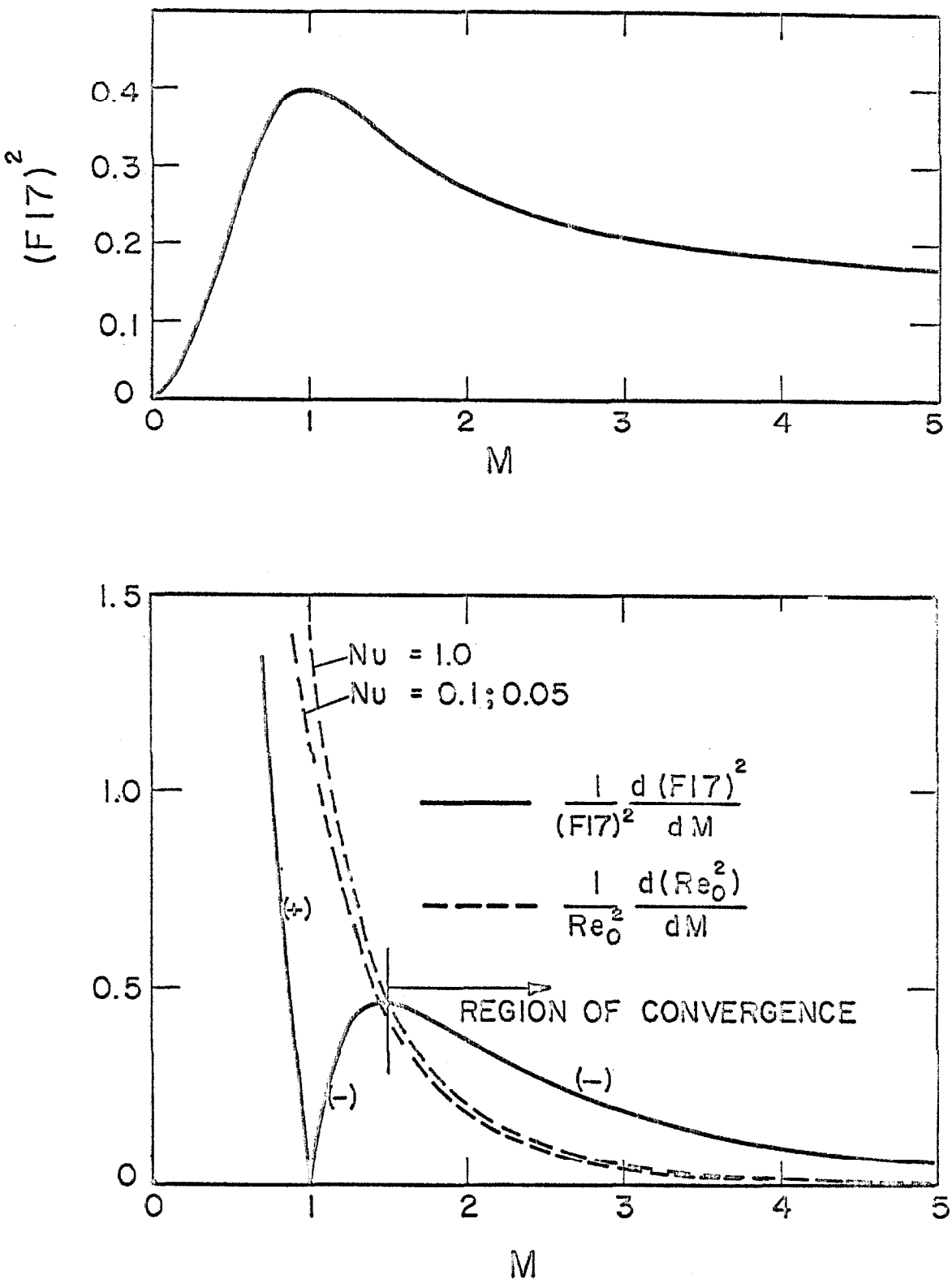


Fig. 19 Variation of Parameters Used in Mach Number Calculation

oscillatory manner above and below the correct value of M. It should be noted that Dewey (12) in reporting an experimental verification for this program used an X/D = 9 wake profile where $2.0 < M < 2.5$.

A quick method of obtaining results from the program as written was to calculate M from pitot-static measurements. This limited the data reduction to a region where the static pressure was reasonably well known which was assumed to be the edges of the wake shear layer. Using this program the calculations converged in an average of 6 iterations.

Behrens* in a review of the approximations made in determining $\psi_N$ discovered an error, and the program was changed to determine $\psi_N$ from the following relations.

$$\psi_{N_{I=0}} = (1 - \omega_o)\left[1 + \frac{st_s}{2}\,\frac{(2\,\omega_o - 1)\,\omega_o - \dfrac{1}{\cosh^2 \nu_o}}{(1 - \omega_o)^2}\right] \qquad \text{(B-3)}$$

$$\omega_o = \frac{\tanh \nu_o}{\nu_o} \qquad \nu_o^2 = \left(\frac{\ell}{d}\right)^2 \frac{k_o}{k_w}\, Nu_o$$

This change increased $Nu_o$ by about 8 percent but had no appreciable effect on $T_*$.

For $M < 0.5$, there was considerable irregular variation in $T_o$ even though $T_*$ was a smoothly varying function. This appeared to be caused by the variation of $\eta_*$. This did not seem reasonable since Stalder, Goodwin and Greager (17) have shown

* W. Behrens, private communication.

$$\eta_f - \eta_c = .2167 \left( \frac{M^{2.80}}{.8521 + M^{2.80}} \right) \qquad \text{(B-4)}$$

which approaches zero as $M \rightarrow 0$.

A check on a couple of data points showed that the computer calculation of $\eta_*$ was larger than $\eta_f$ as calculated by Equation (B-4). This can be attributed to either an incorrect computer program for determining $\eta_f$ or an incorrect relation for $\bar{\eta}_*$. It should be noted that $\bar{\eta}_*$ as determined by the computer program is independent of M even though Dewey's data shows some Mach number dependence for very low M.

There is still a definite need for refinement of the data reduction program if the full potential of the hot wire is to be realized. In rewriting the program attention should be given to choosing parameters which show a minimum sensitivity to the measured variables. In particular only limited reliance on $Nu_m$ should be attempted because of the experimental difficulty in determining this quantity accurately. Consideration should be given to finding a "universal" curve for correlating the heat transfer and recovery factor data. Sherman (16) has suggested the use of Stanton number for the case of subsonic heat transfer from spheres. A similar approach in which $S_t/S_{t_{FM}}$ is plotted against $S_{t_c}/S_{t_{FM}}$ for a cylinder may give a single curve in which $S_t/S_{t_{FM}} = (1 + S_{t_{FM}}/S_{t_c})^{-1}$.

This relationship would prove quite amenable to an iterative solution using a computer program. Consideration could also be given to dividing the program into a low subsonic, transonic, and supersonic regions to take advantage of limiting approximation applicable to each of these regions. No matter what approach is finally taken any computer program needs to be tested over its full range of values before it is considered satisfactory for general use.